UNIVERSIDAD DE INVESTIGACIÓN DE TECNOLOGÍA EXPERIMENTAL YACHAY

Escuela de Ciencias de la Tierra, Energía y Ambiente

TÍTULO: PALEOBOTANY AND STRATIGRAPHY OF THE LOWER APTIAN TO MIDDLE ALBIAN IN THE CENTRAL SUB-ANDEAN ZONE OF ECUADOR

Trabajo de integración curricular presentado como requisito para la obtención del título de Geóloga.

Autor:

Quiroz Cabascango Daniela Elizabeth

Tutor:

PhD. Jorge Toro Álava

Co-tutor:

PhD. Fabiany Herrera

Urcuquí, junio del 2021

Urcuquí, 9 de junio de 2021

SECRETARÍA GENERAL
(Vicerrectorado Académico/Cancillería)
ESCUELA DE CIENCIAS DE LA TIERRA, ENERGÍA Y AMBIENTE
CARRERA DE GEOLOGÍA
ACTA DE DEFENSA No. UITEY-GEO-2021-00001-AD

A los 9 días del mes de junio de 2021, a las 10:00 horas, de manera virtual mediante videoconferencia, y ante el Tribunal Calificador, integrado por los docentes:

Presidente Tribunal de Defensa	Dr. MARTIN MERINO, GERMAN , Ph.D.
Miembro No Tutor	Dr. ALMEIDA GONZALEZ, RAFAEL VLADIMIR , Ph.D.
Tutor	Dr. TORO ALAVA, JORGE EDUARDO , Ph.D.

El(la) señor(ita) estudiante **QUIROZ CABASCANGO, DANIELA ELIZABETH**, con cédula de identidad No. **1004773139**, de la **ESCUELA DE CIENCIAS DE LA TIERRA, ENERGÍA Y AMBIENTE**, de la Carrera de **GEOLOGÍA**, aprobada por el Consejo de Educación Superior (CES), mediante Resolución **RPC-SE-10-No.031-2016**, realiza a través de videoconferencia, la sustentación de su trabajo de titulación denominado: **PALEOBOTANY AND STRATIGRAPHY OF THE LOWER APTIAN TO MIDDLE ALBIAN IN THE CENTRAL SUB-ANDEAN ZONE OF ECUADOR**, previa a la obtención del título de **GEÓLOGO/A.**

El citado trabajo de titulación, fue debidamente aprobado por el(los) docente(s):

Tutor	Dr. TORO ALAVA, JORGE EDUARDO , Ph.D.

Y recibió las observaciones de los otros miembros del Tribunal Calificador, las mismas que han sido incorporadas por el(la) estudiante.

Previamente cumplidos los requisitos legales y reglamentarios, el trabajo de titulación fue sustentado por el(la) estudiante y examinado por los miembros del Tribunal Calificador. Escuchada la sustentación del trabajo de titulación a través de videoconferencia, que integró la exposición de el(la) estudiante sobre el contenido de la misma y las preguntas formuladas por los miembros del Tribunal, se califica la sustentación del trabajo de titulación con las siguientes calificaciones:

Tipo	Docente	Calificación
Presidente Tribunal De Defensa	Dr. MARTIN MERINO, GERMAN , Ph.D.	9,6
Tutor	Dr. TORO ALAVA, JORGE EDUARDO , Ph.D.	9,4
Miembro Tribunal De Defensa	Dr. ALMEIDA GONZALEZ, RAFAEL VLADIMIR , Ph.D.	9,7

Lo que da un promedio de: **9.6 (Nueve punto Seis)**, sobre 10 (diez), equivalente a: **APROBADO**

Para constancia de lo actuado, firman los miembros del Tribunal Calificador, el/la estudiante y el/la secretario ad-hoc.

DANIELA ELIZABETH QUIROZ CABASCANGO Firmado digitalmente por DANIELA ELIZABETH QUIROZ CABASCANGO Fecha: 2021.06.15 11:10:21 -05'00'

QUIROZ CABASCANGO, DANIELA ELIZABETH
Estudiante

Dr. MARTIN MERINO, GERMAN , Ph.D.
Presidente Tribunal de Defensa

GERMAN MARTIN MERINO Firmado digitalmente por GERMAN MARTIN MERINO Fecha: 2021.06.16 08:03:13 -05'00'

Dr. TORO ALAVA, JORGE EDUARDO , Ph.D.
Tutor

CERTIFICACIÓN ELECTRÓNICA BANCO CENTRAL DEL ECUADOR
Firmado Digitalmente por: JORGE EDUARDO TORO ALAVA
Hora oficial Ecuador: 16/06/2021 10:22

Dr. ALMEIDA GONZALEZ, RAFAEL VLADIMIR , Ph.D.
Miembro No Tutor

RAFAEL VLADIMIR ALMEIDA GONZALEZ Digitally signed by RAFAEL VLADIMIR ALMEIDA GONZALEZ DN: cn=RAFAEL VLADIMIR ALMEIDA GONZALEZ, serialNumber=211020132449, ou=ENTIDAD DE CERTIFICACION DE INFORMACION, o=SECURITY DATA S.A. 2, c=EC Date: 2021.06.18 09:24:21 -05'00'

ANDREA YOLANDA TERAN ROSALES

Firmado digitalmente por ANDREA YOLANDA TERAN ROSALES
Fecha: 2021.06.18 08:59:26 -05'00'

TERÁN ROSALES, ANDREA YOLANDA
Secretario Ad-hoc

AUTORÍA

Yo, **Daniela Elizabeth Quiroz Cabascango**, con cédula de identidad 1004773139, declaro que las ideas, juicios, valoraciones, interpretaciones, consultas bibliográficas, definiciones y conceptualizaciones expuestas en el presente trabajo; así cómo, los procedimientos y herramientas utilizadas en la investigación, son de absoluta responsabilidad de la autora del trabajo de integración curricular. Así mismo, me acojo a los reglamentos internos de la Universidad de Investigación de Tecnología Experimental Yachay.

Urcuquí, junio del 2021

DANIELA ELIZABETH QUIROZ CABASCANGO

Firmado digitalmente por DANIELA ELIZABETH QUIROZ CABASCANGO
Fecha: 2021.06.18 10:15:47 -05'00'

Daniela Elizabeth Quiroz Cabascango

CI: 1004773139

AUTORIZACIÓN DE PUBLICACIÓN

Yo, **Daniela Elizabeth Quiroz Cabascango**, con cédula de identidad 1004773139, cedo a la Universidad de Tecnología Experimental Yachay, los derechos de publicación de la presente obra, sin que deba haber un reconocimiento económico por este concepto. Declaro además que el texto del presente trabajo de titulación no podrá ser cedido a ninguna empresa editorial para su publicación u otros fines, sin contar previamente con la autorización escrita de la Universidad.

Asimismo, autorizo a la Universidad que realice la digitalización y publicación de este trabajo de integración curricular en el repositorio virtual, de conformidad a lo dispuesto en el Art. 144 de la Ley Orgánica de Educación Superior.

Urcuquí, junio del 2021

DANIELA ELIZABETH QUIROZ CABASCANGO

Firmado digitalmente por DANIELA ELIZABETH QUIROZ CABASCANGO
Fecha: 2021.06.18 10:16:36 -05'00'

Daniela Elizabeth Quiroz Cabascango

CI: 1004773139

DEDICATION

I dedicate this thesis to my mom Katty because her courage, support, and love were fundamental to my education. I also dedicate this work to my sisters Valeria and Xiomara, their advice, love, and model inspired me to dream.

Daniela Elizabeth Quiroz Cabascango

ACKNOWLEDGMENTS

I want to express my gratitude to my advisor Jorge Toro Álava, for his support and guidance in developing this work. Also, I want to thank my co-advisor, Fabiany Herrera, who, despite the distance, always kept helping me with his comments that were fundamental in this thesis.

My most profound appreciation to my professors Rafael, Anna, Elisa, Celine, Germán, Mateo, Yaniel, and Jorge G. to share their passion and knowledge of earth sciences, and also for teaching me that the ethical values are before academic excellence.

I am very grateful to the Center of Tropical Paleoecology and Archeology, from Smithsonian Tropical Research Institute, especially to Carlos Jaramillo, Mónica Carvalho, Camila Martínez, and Fabiany Herrera to be always predisposed to help me with paleobotany. Especial thanks to Edwin Cadena for instilling in me a genuine curiosity about paleontology.

Finally, thanks to my roommates Andre, Angie, Xiomy, Lady, and Danna for all of the support, advice, and love during five years; and to my geofamily, especially to Nadi, Ariana, Mariela, Harvey, and Jorge. Each of them has helped me enjoy this wonderful experience at Yachay Tech.

Daniela Elizabeth Quiroz Cabascango

RESUMEN

Las paleofloras del Cretáceo de las latitudes bajas de Sudamérica son poco conocidas debido a la falta de investigaciones exploratorias. Actualmente, esta región alberga un alta diversidad de especies de plantas; por tanto, investigaciones de macrofloras Cretáceas, cuya paleo-latitud apenas ha cambiado, pueden dar luz sobre la diversificación inicial de las plantas con flores y coníferas, así como también a los paleoambientes en los cuales se desarollaron los bosques del Cretáceo Temprano de Gondwana.

Recientemente, exploramos el registro paleobotánico y la estratigrafía de la Formación Hollin Inferior, una unidad estratigráfica clástica datada como Aptiano Inferior (?) –Albiano Medio, aflorando en la parte central de la Zona Subandina (SAZ) oriental del Ecuador. Con el objetivo de reconstruir el paleoambiente de la Formación Hollin Inferior, colectamos y estudiamos macrofósiles de plantas, y describimos tres secciones estratigráficas en detalle, de Oeste a Este: Mina Genoveva Abandonada, Mina Genoneva y Afloramiento Pungarayacu.

Las columnas estratigráficas mostraron: areniscas de grano fino a grueso, ricas en cuarzo, masivas y con laminación horizontal, tabular y festonada, formando facies de canal fluvial, barra fluvial, planicie fluvial, interfluvios, pocas facies de planicie y lóbulo deltaico, intercaladas con facies de limolitas y lutitas con laminación horizontal asociadas a depósitos lacustres. Los resultados determinaron un ambiente clástico de depósito fluvial – deltaico – lacustre para la Formación Hollín Inferior, dominado por ríos entrenzados, pequeños deltas y eventos de inundación lacustre.

En los macrofósiles colectados observamos hojas con venación paralela, frondas y cutículas bien preservadas. Con respecto a la probable afinidad taxonómica de los fósiles, se indica la presencia de familias de coníferas como Cupressaceae y Podocarpaceae, helechos como Selaginella, y algunos morfotipos de angiospermas. Además, hay abundante evidencia de ámbar asociado con los macrofósiles de plantas de las secuencias estratigráficas. Así mismo, podemos inferir condiciones húmedas para la depositación de sedimentos arenosos a arcillosos de la formación Hollin, en la actual SAZ central oriental de Ecuador.

De esta manera, nuestros resultados contribuyen al entendimiento de la evolución del cinturón tropical, que hoy en día es la región más diversa del mundo.

***Palabras clave**: paleoflora, Cretácico Temprano, fluvio-lacustre, ámbar.*

ABSTRACT

Cretaceous paleofloras from South American low latitudes are poorly understood due to the scarce research and exploration that has been conducted in these areas. Today, this region holds high plant species diversity; therefore, investigating Cretaceous macrofloras, which paleo-latitude has barely change, can shed light on the initial diversification of flowering plants and conifers as well as on the paleoenvironment in which those Early Cretaceous forests grew in Gondwana.

Recently, we explored the paleobotanical record and stratigraphy of the Lower Hollin Formation, a clastic stratigraphic unit dated as Lower (?) Aptian to Middle Albian, outcropping in the Central Eastern Sub-Andean Zone (SAZ) of Ecuador. Aiming to reconstruct the paleoenvironment of the Lower Hollin Formation, we collected and studied plant macrofossils, and we described three stratigraphic sections in detail, from West to East: Abandoned Genoveva Mine, Genoveva Mine, and Pungarayacu Outcrop.

The stratigraphic columns show massive, horizontal-laminated, through cross-bedded fine- medium- to coarse-grained quartz-rich sandstones forming fluvial channels, fluvial bars, fluvial and interfluvial plains facies, few delta plains, and delta lobe facies, that are interbedded with a few horizontally-laminated siltstones and shales associated to lacustrine facies. The results determine a fluvio – delta - lacustrine clastic depositional environment for the Lower Hollin Formation dominated by braided stream rivers, little deltas, and lacustrine flooding events.

From the macrofossils collected, we observed leaf samples with parallel-venation, fronds, and also well-preserved cuticles. Regarding the probable taxonomic affinities of the fossils, we indicate the presence of conifers families such as Cupressaceae, and Podocarpaceae, fern fronds like *Selaginella,* and a few angiosperms leaf morphotypes. Furthermore, there is abundant evidence of amber associated with the plant macrofossils in the stratigraphic sequences. Moreover, we can infer humid conditions for the deposition of sandy to shaly sediments of Lower Hollin Fm., in the area of the current central Eastern SAZ of Ecuador.

Our results contribute to our understanding of the evolution of the tropical belt, which is today the most biodiverse region in the world.

Keywords: paleoflora, Early Cretaceous, fluvio-lacustrine, amber.

TABLE OF CONTENTS

1 INTRODUCTION

1.1 Relevant Background

The Cretaceous was a period of significant changes for Earth's history. Some of the most remarkable events that took place during this period include: (1) the final breakup of the former Pangea supercontinent; (2) a calcareous nannoplankton and foraminifera explosion creating massive chalk deposits in current northwest Europe, United States, and China; (3) the increase and peak of submarine volcanic activity that enhanced super-greenhouse conditions; (4) the radiation of flowering plants during the Early Cretaceous (Gradstein et al., 2012; Herendeen et al., 2017); and (5) the meteorite impact in the Yucatán Peninsula at 65 Ma (Culver & Rawson, 2004).

Notably, one of these events represents one of the major biotic upheavals in the history of life: the rapid radiation of angiosperms (flowering plants) (Friis et al., 2011). Currently, angiosperms families like Fabaceae, Moraceae, Annonaceae, Euphorbiaceae, Lauraceae, Sapotaceae, Myristicacea, and Arecaceae dominate the multi-stratified, closed canopy, tropical lowland forests representing 50% of the plant diversity (Jaramillo, 2012). This type of forest grows in climatic conditions of annual rainfall of at least 1800 mm and a mean annual temperature between 18ºC and 28ºC (Burnham & Johnson, 2004). The geographical extension of neotropical forests covers from central Mexico to southern Brazil, including Central America, the Caribbean islands, and most of South America (Antonelli & Sanmartín, 2011).

The origin of the neotropical forest remains a mystery (Jaramillo, 2012). The diversity of the neotropical forest is likely the result of several changes along the geologic time. For instance, palynological and paleobotanical data recorded close to K–Pg boundary localities show a great extinction of angiosperms in the latest Maastrichtian, but later gradual recovery of flora in the earliest Paleocene (Nichols & Johnson, 2008). The Early Cretaceous paleofloras from tropical South America are poorly understood due to the lack of scientific research in this region (Burnham & Johnson, 2004) and the difficulty of recovering well-preserved fossils in areas that are currently covered with abundant vegetation.

Previous studies on macrofossil plants from South America indicate a strong dominance of gymnosperms such as cycads, conifers, Bennettitales, and ferns, while early angiosperms are only a minor component (Lima et al., 2012; Martínez et al., 2020; Mejia-Velasquez et al., 2018; van Waveren et al., 2002). In Ecuador, the only previous study of Early Cretaceous macrofloras was done by Schoemaker (1982) in the southwest of this country. This author studied the flora from the Aptian-Albian Ciano Formation and described only a few fossil gymnosperms and ferns.

1.2 Problem Statement

There are few studies of Early Cretaceous macrofloras in low latitude South America (Figure 1). Most of them have been conducted in Colombia and Peru, and Brazil. Ecuador has only one study, whereas Venezuela, Bolivia, and Paraguay have none. These countries belong to the Neotropic, which is well-known because of the large number of the world's living species (Burnham & Johnson, 2004). Therefore, the recovery of angiosperms and other groups of plants (i.e., conifers, ferns, ferns allies, etc.) will significantly contribute to understanding tropical forest evolution.

The only way to prepare ourselves against future climatic changes is by studying how organisms responded to past changes. Hence, sedimentology, micropaleontology, paleobotany, palynology, and geochemistry analyses are critical to developing paleoecological reconstructions (Battarbee et al., 2002; Dark, 2008; Holmes, 2001; Nichols, 2009; Shuman, 2013) that can allow us to use the past as a guide for the future.

The Hollin Formation is the stratigraphic unit that will be studied in this thesis research project. This unit is traditionally known as Lower Hollin Formation. Many studies have been conducted in the Hollin Formation because of its oil reserves. Nevertheless, little is known about the lower part of the Hollin Formation due to the lack of large oil deposits and, consequently, minimum industrial interest (J. Toro, personal communication, January 21, 2021). A reconstruction that explains the paleoecological and depositional conditions of the Lower Hollin Formation is also essential for understanding the floristic composition of neotropical forests.

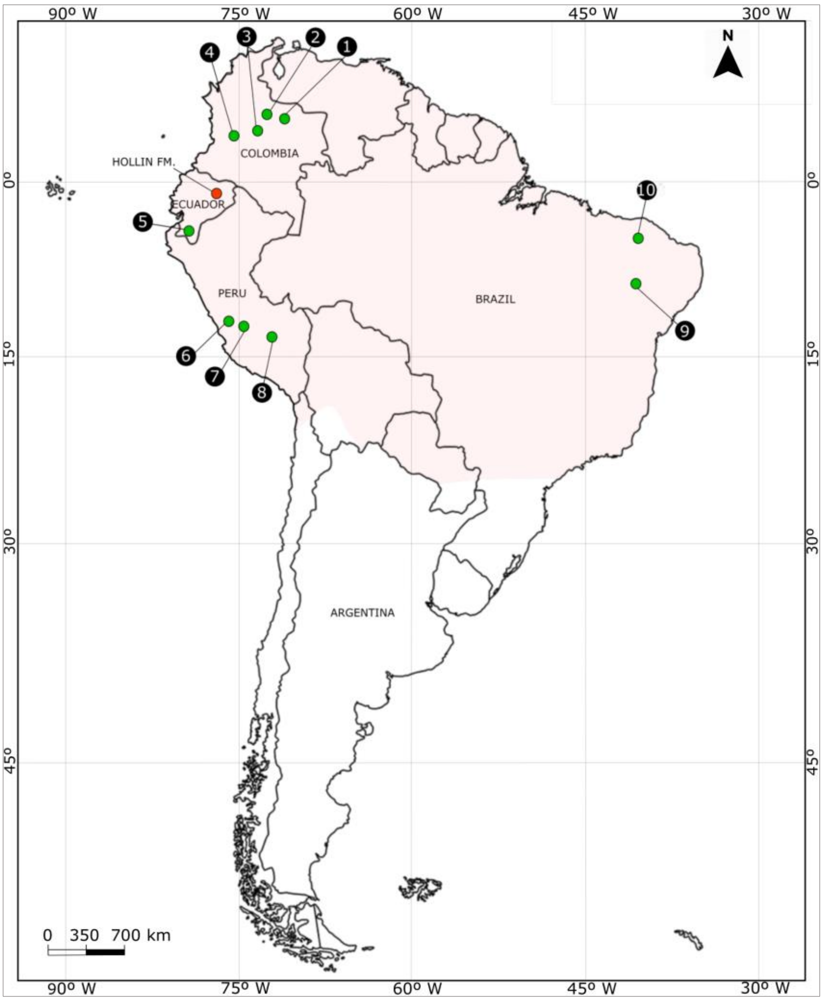

Figure 1. Most studied/important tropical South American palaeofloras of Early Cretaceous age. The zone in pink represents tropics. The red dot represents the location of this study. The green dots represent the locations of previous studies: 1) Páramo de Chita. 2) Villa de Leyva. 3) Río Upín and Río Bata. 4) Valle Superior del Magdalena. 5) Puyango. 6) Lima surroundings. 7) Huallanca. 8) Huancané Fm. 9) Crato Fm. 10) Paranaiba. Modified after Martínez et al. (2020).

1.3 Objectives

1.3.1 General Objetive

The primary purpose of this research project is to contribute to a better understanding of the neotropical forest evolution at the low latitude South America through the reconstruction of a paleoenvironment of two new Early Cretaceous localities corresponding to the Aptian-Albian Lower Hollin Formation from the Central Eastern Sub-Andean Zone (SAZ) in Napo province, Ecuador.

1.3.2 Specific Objectives

- To describe the stratigraphic sections from two Early Cretaceous localities in central SAZ based upon its lithology, bedding styles, and sedimentary structures to establish the paleo depositional environments of these localities.
- To define morphotypes and identify the vegetation groups of leaf macrofossils and cuticle remains.
- To characterize the amber clasts, present in the study area.

2 GEOLOGICAL FRAMEWORK

2.1 Outcrop Locations

The study area is located in the Central Eastern SAZ of Ecuador, at the western side of the Oriente Basin, in the Lower Hollin Formation. It can be accessed through the Baeza - Tena road, Napo province.

For this study, three places were considered within the Archidona canton: (1) the Genoveva Mine, (2) abandoned Genoveva Mine, and (3) the Pungarayacu outcrop, just to the east of the Pungarayacu quarry. These three localities limit to the North with the Sumaco National Park, the West with the Jondachi parish, and the South with the Osayacu parish, the latter two part of the Archidona canton in Napo province (Figure 2).

The Genoveva mine belongs to the Narupa commune, Cotundo parish, of the Archidona canton. It is located at 600 meters northwest of the intersection of the Loreto – Coca road with the main road that connects Baeza with Tena, at the geographical coordinates 0°42'42.73"S, 77°47'17.83"W. It can be accessed following an asphalted third order road. At the moment, the Genoveva mine, from which quartz-rich sands are extracted, has two exploitation fronts, only one of them being active. On the other hand, the Pungarayacu outcrop is located in the Cotundo parish, of the Archidona canton. It is located at 10 km east from the intersection of the Loreto – Coca road and Baeza - Tena road, at the geographical coordinates 0°42'23.93"S, 77°44'31.81"W. It can be accessed following the Loreto – Coca road, at 250 meters of the Pungarayacu Quarry (Figure 2).

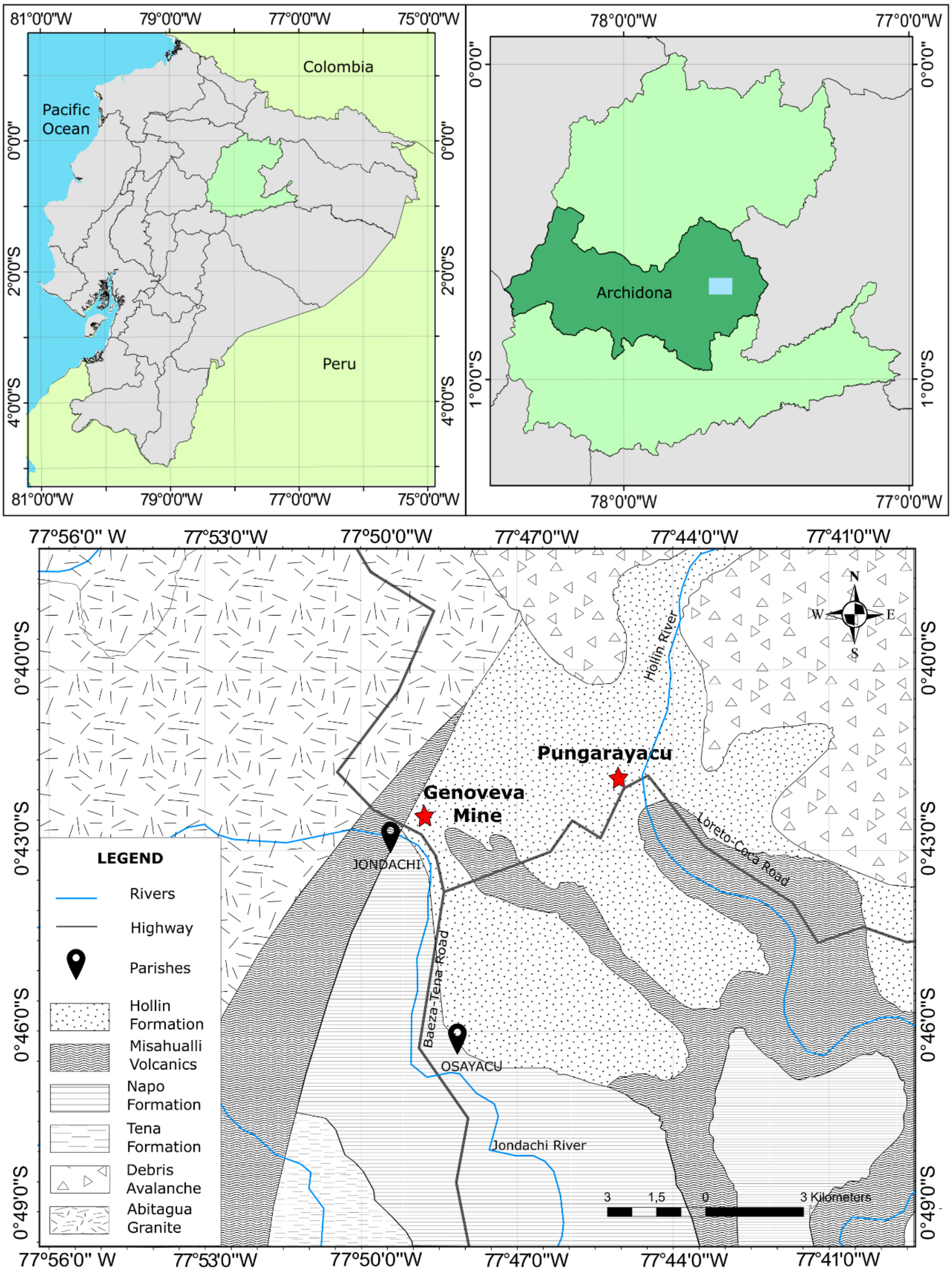

Figure 2. Location map of the studied area.

2.2 Regional Background

The Oriente Basin of Ecuador forms part of the Sub-Andean retro-arc foreland basin system, which consists in the actual foredeep (Oriente Basin) and the Subandean Zone (Napo and Cutucu uplifts) between the Putumayo Basin of Colombia and the Marañon Basin of Peru (Christophoul et al., 2002). The study area is located in the uplifts of the western part of the Oriente basin, specifically in the Sub-Andean Zone. This area shows an evolution from an epi-cratonic basin (Lower Hollin Sandstone, Napo Basal, Lower Napo, Medium Napo) to a foreland basin (Upper Napo Formation, Tena Formation, and Tiyuyacu Formation) (Baby et al., 2004).

2.3 Stratigraphy

The SAZ is the westernmost and proximal part of the Oriente Basin, where Paleozoic basement, Mesozoic–Cenozoic volcanic rocks, and sedimentary units are exposed (Vallejo et al., 2002). One of these units and the most studied is the Hollin Formation because it is the principal oil reservoir in the Oriente Basin (Dashwood & Abbotts, 1990). It outcrops in nearly all of the Amazonian provinces of Ecuador. The spatial distribution of the Hollin Formation spans from the South of Colombia in the Putumayo Basin to the North of Peru in the Santiago Basin and Marañon Basin (Romero Condor, 2018). It is generally accepted that Hollin Formation has Aptian to Albian in age (Baby et al., 2004; Vallejo et al., 2002; White et al., 1995). Villagomez et al. (1996) confirmed the SW to NE diachronism of Lower Hollin Formation; and, as a result of a widespread macro- and micro-paleontological study, the Lower Hollin Formation received an age interval of Lower Aptian (?) – Middle Albian (Jaillard et al., 1997). However, Ruiz (2002) opened the possibility the Lower Hollín Fm. being older than early Valanginian to late Barremian.

The Hollin Formation was first defined as sandstones by Wasson & Sinclair (1927). Then, it was formally described by Tschopp (1953) as coarse, porous, and blanket sandstone, thick-bedded to massive, with cross-stratification and sporadic ripple marks. The bedding planes are filled by thin intercalations of micaceous shales, dark sandy silts, and black coaly shales at the top of this stratigraphic succession. These sediments rest on an angular unconformity over pre-Cretaceous volcanic and volcanoclastic substratum.

The Hollin unit comprises two formations as usually recognized in the oil industry, the Lower Hollin Formation, known as the Main Hollin Sandstone (Baby et al., 2004), and the Lower Sandstone, known as the Upper Hollin Sandstone or Upper Hollín Formation (Jaillard et al., 1997).

According to White et al. (1995), the Lower Hollin Formation can be divided into three depositional systems, from bottom to top: (1) The basal part that comprises sandstone channels and flood basin shales which are interpreted as paleovalley fluvial deposits; (2) Next, a package composed of three facies: first, a planar and trough cross bed sets interpreted as straight and sinuous-crested mid-channel bars; second, interbedded of sandstones and mudstones attributed to channels, and overbank levees; and third, a thick mudstone package inferred as channel abandonment and flood basin deposits. These sedimentary facies were developed in a braided alluvial plain system; and (3) Coastal plain: the last depositional system of the Lower Hollin Formation composed of planar to trough cross-bedded fining-upward sandstones and thin rhythmic mudstones inferred as a meandering stream system.

The Upper Hollin Formation is composed of two depositional systems that have been interpreted as marine deposits that transgressively overlie the Lower Hollin Formation. White et al. (1995) describe as follows: (1) the Shore zone depositional system composed by a planar to through cross-bedded fine to medium-grained quartzitic sandstones, very fine to fine-grained ripple laminated sandstones, and burrowed lenticular-bedded mudstones, interpreted as sand-dominated bayhead deltas, estuaries, subtidal shoals, and muddy tidal flat; and (2) an Open marine depositional system with lithofacies consisting of glauconitic and quartzose sandstones, well-lithified limestones and marls, and shales including trough cross-bedding, ripple lamination, and flaser bedding. In the Upper Hollin, the basal quartzitic sandstones and shales are interpreted as a subtidal shoal while the fossiliferous, micritic limestones and marls record the final stage of Hollin deposition showing a sea transgression eastward over the Cretaceous Oriente margin (White et al., 1995).

Other studies also define the general depositional environment in the Lower Hollin. Smith (1989) proposed a transition from dominantly fluvial to a fluvial-deltaic environment, and other authors (Romero Condor, 2018; Shanmugam et al., 2000) suggest a tide-dominated estuarine instead of a fluvial-deltaic environment. Baby et al. (2004) propose that the Hollin Formation is a clastic deltaic-estuarine system covered by shallow marine platform facies, and the upper part is a succession of limestones, calco-sandstones, glauconitic sandstones, and shales from a marine environment representing the Highstand Systems Tract (HST) of the first Hollín-Napo sedimentary cycle.

3 PALEOBOTANICAL FRAMEWORK

3.1 Review of fossil macrofloras from the Early Cretaceous of tropical South America.

During the Triassic and Jurassic, global forests were dominated mainly by Coniferales, Filicopsids, Cycadales, and Bennetitales, and at a minor rate by Ginkgoales, Pteridosperms, Sphenopsids, and Lycopsids (Willis & McElwain, 2014). Later, during the Early Cretaceous, flowering plants (angiosperms) began to take a leading role (Romero, 1993). They rapidly diversified worldwide by the Late Cretaceous (Cenomanian to Campanian, 99–70 Ma), being floristically dominant in middle and high latitudes of the Northern hemisphere (Mejia-Velasquez et al., 2012).

The Aptian-Albian interval is characterized by both high tropical temperatures (~ 31 °C) and high levels of CO_2 (~ 1000 ppm) (Schouten et al., 2003; and Breecker et al., 2010; *in*: Mejia-Velasquez et al., 2012). Nonetheless, Herngreen (1996) proposed that low tropical latitudes in northern Gondwana were arid during the Albian-Aptian interval. Other authors have proposed humid conditions for the tropics during the Albian, almost doubling modern precipitation values at low latitudes based on data and models from oxygen isotopes of pedogenic carbonates that show an intensification of the hydrological cycle ((Ziegler et al., 1987; Ufnar et al., 2004; Suárez et al., 2010; *in*: Mejia-Velasquez et al., 2012).

Below, from North to South, we will review previous research results of plant macrofossils of northern South America (See Table 1) during the Early Cretaceous.

3.1.1 Venezuela

Few plant remains were reported from the Barranquin Formation, which has led to the prevailing opinion that this formation is continental in origin. These plants were studied by Schlagintweit (1919), who identified *Weichselia manlelli*, and by Dietrich (1924), who reported *Olozamites* and *Equisetiles*. However, their stratigraphic data are meager and inconclusive. Therefore, many of these plant remains can be marine algae rather than land plants (Von Der Osten, 1957).

3.1.2 Colombia

From the Early Cretaceous of Colombia, several fossil plants have been collected near the Villa de Leiva town (see Figure 1) that belong to the Pteridophyta, Cycadophyta, Coniferophyta, and two, not well-defined taxa, presumably angiosperms (Huertas, 1970; van Waveren et al., 2002). Moreno Sánchez (2007) described two characteristic genera of the Cheirolepidiaceae collected from Aptian-Albian marine beds in Bucaramanga, Villa de Leiva, and Aipe localities. In 2016, Monje-Dussán *et al.* reported new lower Aptian – Albian plant macrofossils associated with filicopsids and conifers collected in the Upper Magdalena Valley Basin in three exposed levels of the Yaví and Caballos Formations.

3.1.3 Ecuador

There are barely any Cretaceous macroflora studies in Ecuador. The only research was developed by Schoemaker (1982). He reported a detailed study of fossil leaves collected in the Ciano Formation, from the Early Cretaceous, in the southern part of Ecuador. The fossils include mostly Cycadales, followed by Bennettitales and Conifers (including Pinales).

The first hint of Early Cretaceous plant remains of the Hollin Formation was in an oil exploration industrial report by Tschopp (1953). Subsequent authors (Mariño Morejón, 2016; Shanmugam et al., 2000; White et al., 1995) indicated the presence of plant remains in several Hollin facies, but they had not been the object of interest because these studies were more focused on hydrocarbon prospection. Cadena et al. (2018) reported for the first time well-preserved small seeds and cuticle remains recovered from the Pungarayacu quarry (Hollin Formation). All of them noticed amber remains, from granular coarse grains to pebbles.

3.1.4 Perú

In the Berriasiane – Valanginian stages of southern Perú, the Huancane Formation has abundant conifers fossil leaves, with the following taxa: *Brachyphyllum, Podozamites, Cupressinocladus, Araucarites,* and other leaves of Araucariales affinity (Martínez et al., 2020) (Figure 1). Furthermore, wood and fruit samples with probable affinity to *Lecythidaceae, Malvaceae, and Arecaceae* were reported from Colombia, Peru, and Brazil, but their affinities remain obscure (Burnham & Johnson, 2004).

3.1.5 Brazil

In Northeastern Brazil, Araripe Basin is best known for its well-preserved fossil record of flora and fauna (Lima et al., 2012). Its paleoflora is abundant, dominated by conifers, some lycopsids, ferns, and gnetalean plants of unknown affinity, including angiosperms. In general, gymnosperms represent the most abundant group. There are reports of paleoflora in the Crato Formation, which belongs to Araripe Basin, that have not been studied in detail, but include roots, stems, leaves, and fruiting bodies of a variety of pteridophytes, gymnosperms, cycads, gnetaleans, and angiosperms (Martill et al., 2005). Mohr & Friis (2000) also indicate several angiosperm remains that correspond to the magnoliid clade (Figure 1).

Table 1. Selected Early Cretaceous macrofloras from low latitude South America.

Country	*Locality*	*Macrofloras*								
		Cycads	Bennetittales	Conifers	Ferns	Lycopsid	Gnetales	Angiosperms	Equisetales	Pinales
Venezuela	Barranquin Formation *(Von Der Osten, 1957)*						X		X	
Colombia	Villa de Leiva *(van Waveren et al., 2002)*	X		X	X			X		
Colombia	Bucaramanga, Villa de Leiva and Aipe *(Moreno Sánchez et al., 2007)*			X						
Colombia	Upper Magdalena Valley Basin *(Monje-Dussán et al., 2016)*			X	X					
Ecuador	Ciano Formation *(Schoemaker, 1982)*	X	X	X						X
Peru	Huancane Formation *(Martínez et al., 2020)*	X		X						
Peru	*(Burnham & Johnson, 2004)*							X		
Brazil	Araripe Basin (Lima et al., 2012)			X			X			
Brazil	Crato Formation *(Martill et al., 2005*)	X		X			X	X		
Brazil	Crato Formation *Mohr & Friis (2000)*							X		

3.2 Cuticles and Stomata

The cuticle, which can be defined as an extracellular hydrophobic layer that covers the aerial epidermis of all land plants, was developed in response to different challenges that the plants were subjected such as desiccation and external environmental stresses (Yeats & Rose, 2013) (Figure 3A). Therefore, some fundamental functions of cuticles are the protection against water loss, regulation of gas exchange, protection against the attack of microorganisms or pests, and increased exposure to UV radiation (Domínguez et al., 2011).

The occurrence of cuticles in the fossil record has significant implications due to the well-preserved information of stomatal complex and epidermal cells. The stomatal complex constitutes the stoma and the surrounding cells that participate in the closing and opening of the pore. The stoma can be defined as the pair of guard cells and the pore enclosed (Van Cotthem, 1970). Through it, plants can control the exchange of water vapor, as well as carbon dioxide and oxygen (Crang et al., 2018).

According to Van Cotthem (1970), several types of stomata have been defined (Figure 3B):

- Anomocytic. The stoma is surrounded by a limited number of cells that are indistinguishable in size or form from those of the remainder epidermis.
- Anisocytic. The stoma is surrounded by three cells, of which one is distinctly smaller than the other two.
- Diacytic. The stoma is enclosed by a pair of subsidiary cells whose common wall is at right angles to the guard cells.
- Actinocytic. The stoma is surrounded by a circle of radiating cells.
- Paracytic. The stoma is accompanied either side by one or more subsidiary cells parallel to the long axis of the pore and guard cells.
- Tetracytic. Guard cells are surrounded by four subsidiary cells, two lateral and two polar ones.
- Cyclocytic. The stoma is surrounded by four or more subsidiary cells forming a narrow ring around each stoma.

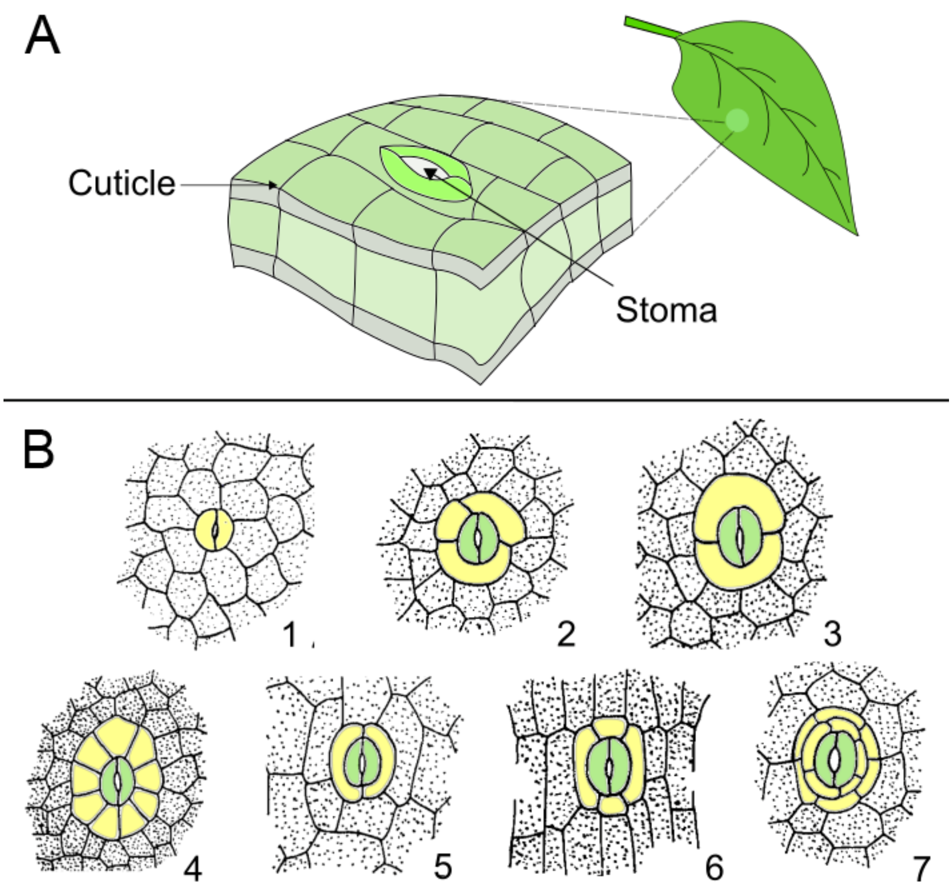

Figure 3. A) Graphic representation of the stoma and the cuticle. B) Stomatal types and their new technical terms. The guard cells are green in color, the subsidiary cells are yellow, and the epidermal cells are grey. 1. Anomocytic; 2. Anysocytic; 3. Diacytic; 4. Actinocytic; 5. Paracytic; 6 Tetracytic; 7. Cyclocytic. Modified after Van Cotthem (1970).

4 METHODOLOGY

Several field trips were carried out to the Pungarayacu Outcrop, to the Genoveva Mine and surroundings, and the abandoned Genoveva Mine, in order to construct stratigraphic columns (graphic logs) and to collect rock samples and plant macrofossils for further analysis and interpretation.

The field trips were carried out during 2018-2020. The first was conducted in 2018 by Dr. Edwin Cadena and collaborators, who collected rock samples that contained plant remains from Pungarayacu Quarry. The second field trip, in January 2020, was organized between the researchers Dr. Carlos Jaramillo and Dr. Camila Martínez from the Smithsonian Tropical Research Institute, Dr. Fabiany Herrera from the Chicago Botanic Garden and Dr. Jorge Toro Álava of Yachay Tech University. We visited the Genoveva Mine and surrounding localities in this field trip, collecting and analyzing plant macrofossils and amber clasts. Finally, the third and last field trip was done in October 2020 under the direction of Dr. Jorge Toro Álava, in which we finished the description of the Pungarayacu section and collected rock samples.

4.1 Stratigraphic Columns

Stratigraphic columns (graphic logs) were developed during the referred field trips. They were constructed at a scale of 1:150 and described in detail several factors as lithology, sedimentary structures, bedding and laminations, fossil content, oil staining, and paleocurrents.

Later, at the office, they were digitalized using SDAR Package of R (Jaramillo, C., & Ortiz, J., 2020) and edited in Adobe Illustrator CS6. The collected data in the graphic logs allowed us to interpret sedimentary facies and the paleoenvironment of deposition.

Besides, a MAVIC PRO drone (number series: 08QCE9V0225Z4E) was employed to acquire digital images of the vertical wall of the Genoveva Mine to interpret sections that were inaccessible in person.

The sediment transport direction was measured, taking into account the plane generated by the cross-stratification, and the direction which is parallel to the perpendicular axis to the horizontal plane. These measurements were taken in sub-horizontal layers and were later interpreted through rose diagrams in order to estimate the direction of the flow.

4.2 Fossil Cuticles

The following procedure was applied to isolate fossil cuticles from bulk sediment samples:

4.2.1 Isolation

Samples were allowed to air dry at ambient temperature and were manually disaggregated with a hammer to reach 5-10 cm size. The resulting rock fragments were placed in a beaker with hydrogen peroxide at 7% concentration and a magnetic stirrer on a plate for up to 3 days. This resulted in the complete disaggregation of rock samples. When the sediment was settle, the residual hydrogen peroxide was separated, and sediment samples were thoroughly rinsed with water. The sediment samples were allowed to dry on a hot plate at 100˚C for 30 minutes and were subsequently sieved by grain size using a strainer.

After that, the sediments recovered were observed under Olympus SZX16 Stereo Microscope. Cuticle fragments were manually picked and mounted with glycerin jelly on glass slides. The cuticle samples included fragments of the upper and lower epidermis of leaves and seeds. A total of twenty-five samples were separated and are housed in the paleontological collection of Yachay Tech University.

4.2.2 Photography

The mounted specimens on glass slides were observed under epifluorescence using an Olympus DP73/BX63 Microscope and Nikon Eclipse E600 Microscope with a halogen light source. Using epifluorescence takes advantage of the auto-fluorescent properties of cuticles and improves the resolution of the epidermal pattern. Samples were observed under a confocal Olympus Fluoview FV1000 microscope to see specific details of stomas or epidermal cells.

4.2.3 Cuticle Analysis

Cuticle samples were separated into morphotypes based on the morphological characteristics of the epidermis. The features considered were morphology of guard, subsidiary and epidermal cells, and the distribution of stomata.

4.3 Leaf Macrofossils

Most of the leaf macrofossils were recovered *in-situ* in the outcrop of the abandoned Genoveva Mine. These specimens were transported to the Chicago Botanic Garden, United States, for further analyses. Fossils were photographed using a Canon Rebel camera with 100 mm macrolens attached to a Stackshot system, and digital images were merged using Helicon Focus software (USA). Plates were constructed using Photoshop 6.0.

5 RESULTS

5.1 Stratigraphic Results

Three stratigraphic columns were constructed from the Pungarayacu area, Genoveva Mine, and abandoned Genoveva Mine. The lithofacies were described following Miall (1978) (see Table 5), taking into account the lithology, sedimentary structures, bedding, amber content, plant remains, and coal. Base on that, sedimentary facies were established and the paleo-environment interpreted.

5.1.1 Pungarayacu Outcrop

The Pungarayacu outcrop is located east of the Pungarayacu quarry. The stratigraphic log of the Pungarayacu outcrop was described in a limited access area due to both the vegetation coverage (Figure 4B) and the steep outcrop surface. Therefore, the description was made along 180 meters of Loreto – Coca road cuts. Sub-horizontal and tilted layers constitutes the Pungarayacu Outcrop (Figure 4A and 4C), the last help to describe the total thickness of the stratigraphic log reaching 42 meters (Figure 6).

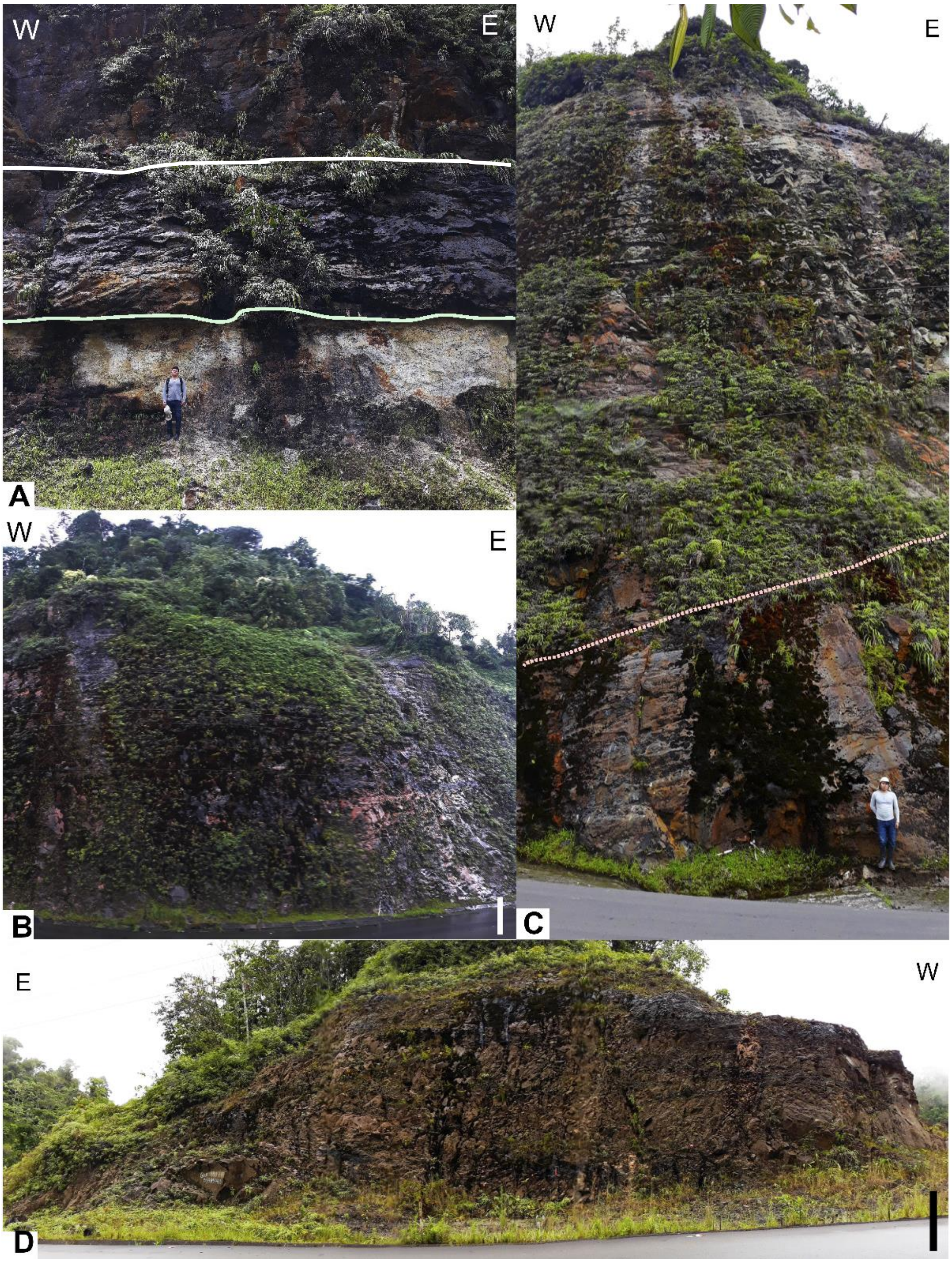

Figure 4. Outcrops in the Loreto – Coca road at 200 meters East from the Pungarayacu Quarry. A) Bottom line mark the boundary between Lower Hollin Formation and the underlying Misahualli Volcanics. Also it shows sub-horizontal sandstone package. Outcrop location -0,71111º S; -77.7394º W. B) Vegetated covered outcrop located at -0.7119444º S; -77.740833º W. Scale bar 2 meters. C) Typical tilted sandy package located at -0.7125º S; -77.74º W. D) Sandstone outcrop located at -0.7116667º S; -77.740833º W. Scale bar 2 meters.

Nine lithofacies, corresponding to ten depositional sub-environments and five major environments (Table 2), were defined. The lithofacies are: Through cross-bedded sand (*St*); Planar-cross-bedded sand (*Sp*); Ripple cross-laminated sand (*Sr*); Horizontally-bedded sand (*Sh*); Massive sand (*Sm*); Siltstone, silty claystone or claystone, horizontally laminated to massive (*Fsc);* laminated sand, silt and mud *(Fl)*; Paleosoil (*Pl*); and Pyroclastic flow (*Pf*).

The depositional sub-environments are, from deepest to shallowest: Outer lake, Bay, Beach (Shoreline), Mouth bar, Fluvial plain, Overbank, Fluvial Bar, Fluvial Channel, Distal Alluvial Fan, and Pyroclastic flow.

Major environments identified in the Pungarayacu outcrop, from deepest to shallowest, are Lake, Shoreline, Braided Stream River, Alluvial Fan, and Volcanoclastic.

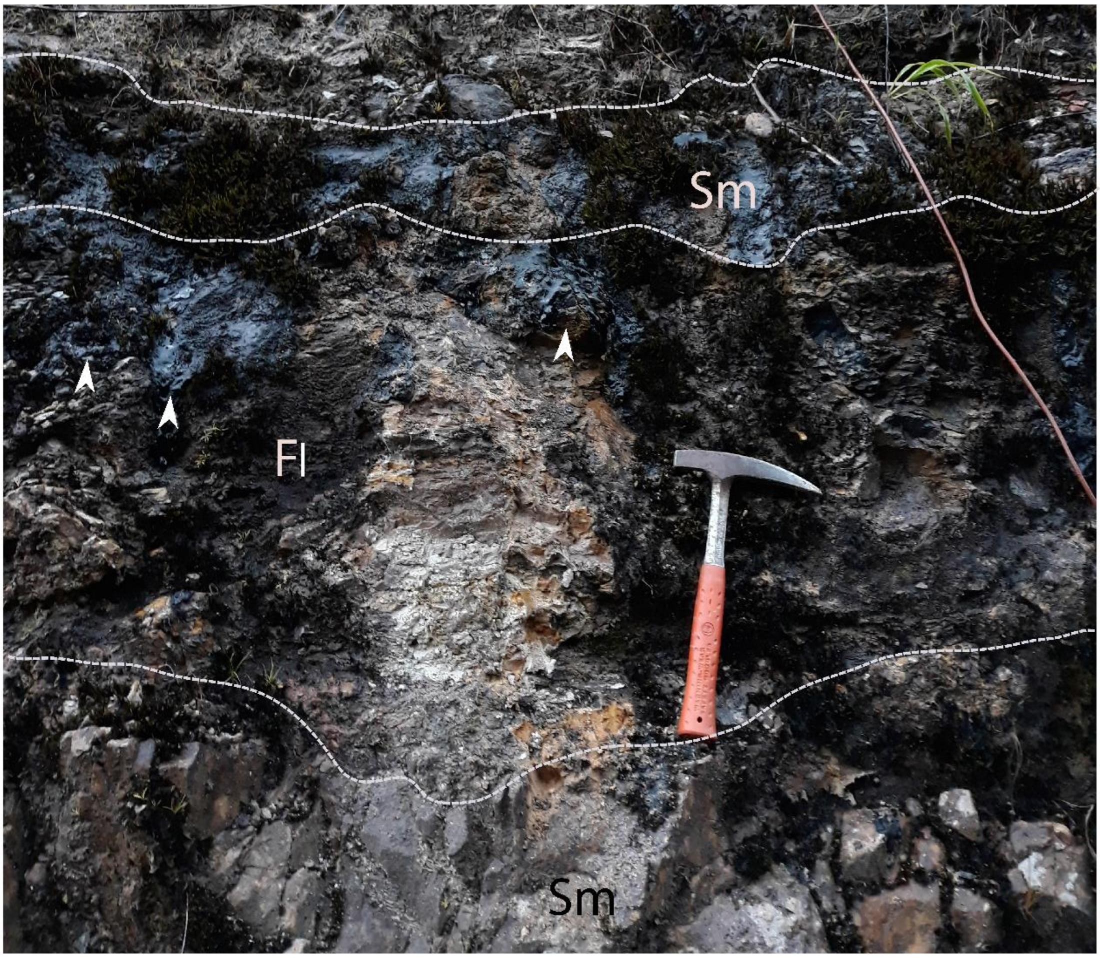

Figure 5. Lithofacies in Pungarayacu stratigraphic log. Lithofacies *Fsc* corresponding to bed 57 in Figure 6, which contains plant remains in horizontal lamination; *Sm*, massive quartz-rich partially oil-stained (white arrows) sandy bed. Scale bar: hammer 32.5cm long.

No complete plant macrofossils were found in the Pungarayacu outcrop area; however, one package of siltstones contain a few cuticle remains. The bed 57 corresponding to the *Fl* lithofacies, assigned to the overbank deposits, record the first plant remains in the Lower Hollin Formation (Figure 6). The parallel-laminated and ripple laminated siltstone is interbedded with medium-grained sandstones (Figure 5). The upper *Sm* has weak oil staining and exudes viscous tar.

Table 2. Lithofacies, sedimentary structures and depositional sub-environments identified at of Pungarayacu Outcrop employing the Miall (1978) code

Lithofacies	***Description***	***Amber***	***Plant remains***	***Coal & organic debris***	***Bed Numbers***	***Depositional Element***
Sm	Massive very fine sandstone.				76,77,78	Bay
Fsc	Parallel-laminated siltstone.				83	Outer - Lake
Sh	Parallel-laminated fine sandstone.				80,81,82	Beach - Inner Lake
Sm	Massive fine sandstone.				68,84	Beach
Sh, *Sm*	Parallel-laminated fine sandstone; massive very fine sandstone.				72,73,74,75,79	Beach – Fluvial Plain
Fsc, *Sp*, *Sh*	Massive siltstone; fine planar cross-stratified sandstone; parallel-laminated medium sandstone.				11,12	Fluvial Plain
Fl	Massive siltstone; parallel-laminated siltstone with ripples, coal layers and plant remains.		X	X	5,20,57,59,61,63,65,66, 67,69,70,71	Overbank
Sm	Massive fine to medium sandstone.				62	Mouth Bar
Sp, *Sr*, *Sm*, *Sh*,	Planar cross-stratified medium sandstone with ripple marks; massive coarse sandstone; parallel-laminated fine sandstone.				3,4,7,8,9,10,21,22,23,28, 29,30,32,33,44,45,48,52, 53,54	Fluvial Bar
Sm, *Sp*, *Sr*, *St*,	Massive fine sandstone with concretions; planar cross-stratified medium sandstone with ripple marks; through cross-laminated fine sandstone.				6,13,14,15,16,17,18,19,24, 25,26,27,34,35,36,37,38,39 ,40,41,42,43,46,47 49,50,51,56,58,60,64	Fluvial Channel
Sh	Parallel-laminated coarse sandstone.				2	Distal Alluvial Fan
Pl, *Pf*	Poorly consolidated weathered ash matrix (60% matrix and 40% of clasts). The color is variable from pink, reddish, gray and light green. The mineralogical content is mostly Plagioclase, K-feldspar and Quartz. Sequence boundary surface at the top is N10ºW/11ºNE.				1	Pyroclastic Flow

Graphic Log of Pungarayacu

Scale 1:150

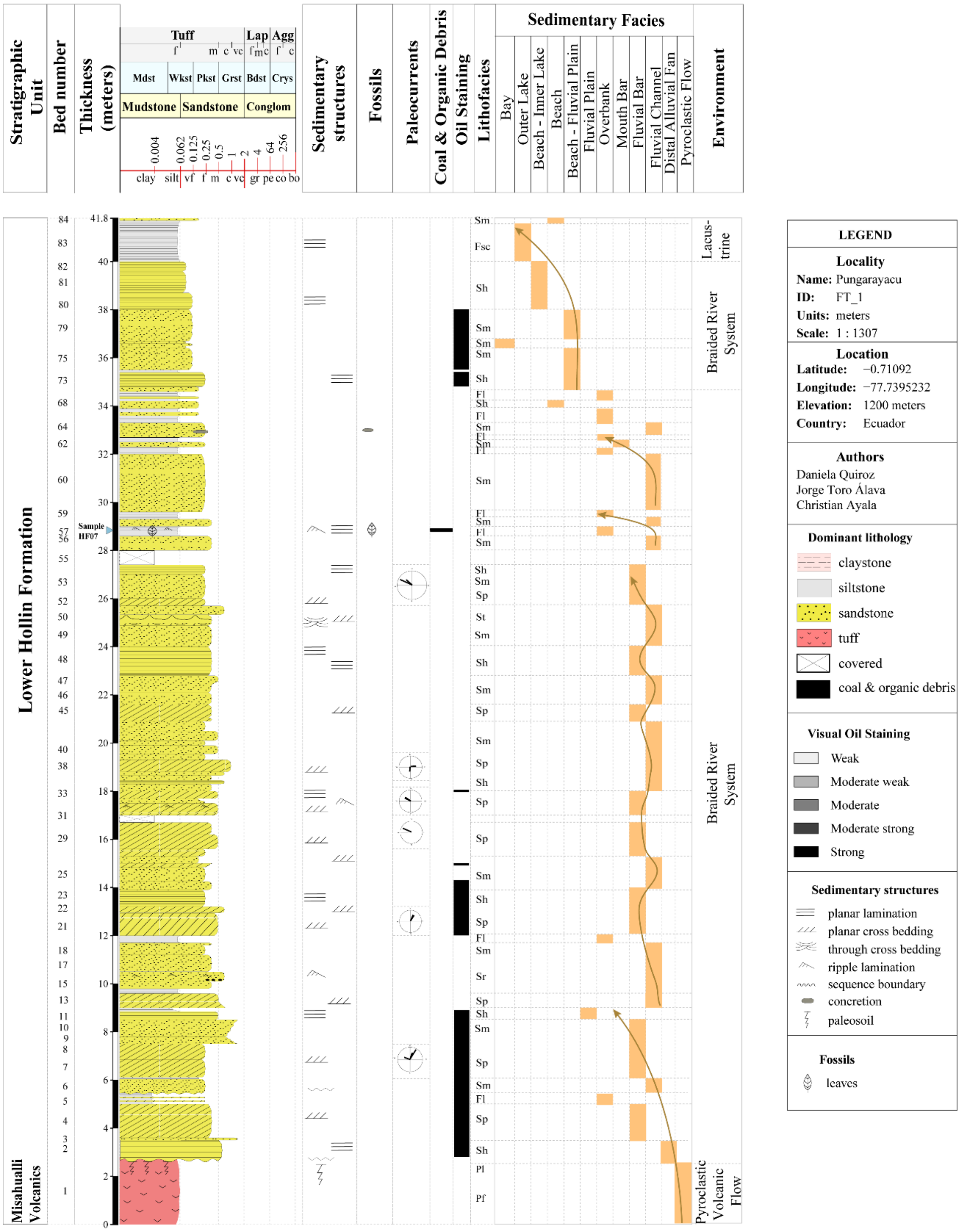

Figure 6. Stratigraphic Log of Pungarayacu Outcrop. See detail in Annex 1.

5.1.2 Genoveva Mine.

In order to build the stratigraphic log of Genoveva Mine, three sections were defined: (1) the first one was described from the Hollin subsidiary river to the top of the waterfall (Figure 7D); (2) the second section was built in the ravine above the waterfall (Figure 7E); and (3) the third section was constructed in the active zone at the Genoveva Mine (Figure 7A-C). The digital elevation model was made by Mauricio Baquero and Rafael Castaño, collaborators from the Smithsonian Tropical Research Institute, using the MAVIC PRO drone (number series: 08QCE9V0225Z4E). The stratigraphic column reached a total height of 72.5 meters (Figure 10).

Ten lithofacies and eleven depositional sub-environments were identified in the Genoveva Mine (see Table 3). These lithofacies are: Through cross-bedded sand (*St* - Figure 9A); Planar cross-bedded sand (*Sp* - Figure 8D); Ripple cross-laminated sand (*Sr*); Horizontally-bedded sand (*Sh* - Figure 8C); Massive sand (*Sm* - Figure 9A); Horizontally-laminated to massive siltstone, silty claystone or claystone (*Fsc* – Figure 9C); laminated sand, silt and mud *(Fl);* Coal (*C* - Figure 8B); Paleosoil (*Pl*); and Pyroclastic flow (*Pf*). Furthermore, there are rip-up clasts (Figure 9B) in beds number 40,41,49 of stratigraphic log (Figure 10) within massive medium to fine-grained sands.

Several plant macrofossils were recovered from siltstone levels (see point 5.2.2): Amber (Figure 26), Coal layers (Figure 8B), and concretions in siltstone and sandstone packages.

Eleven depositional sub-environments were identified, from deepest to shallowest: Outer lake, Middle lake, Inner lake, Bay, Hyperpycnal flow, Fluvial plain, Overbank, Fluvial Bar, Fluvial Channel, Interfluvial Channel, and Pyroclastic flow.

Major environments identified in the Genoveva Mine, from deepest to shallowest, were Lake, Braided Stream River, and Volcanoclastic.

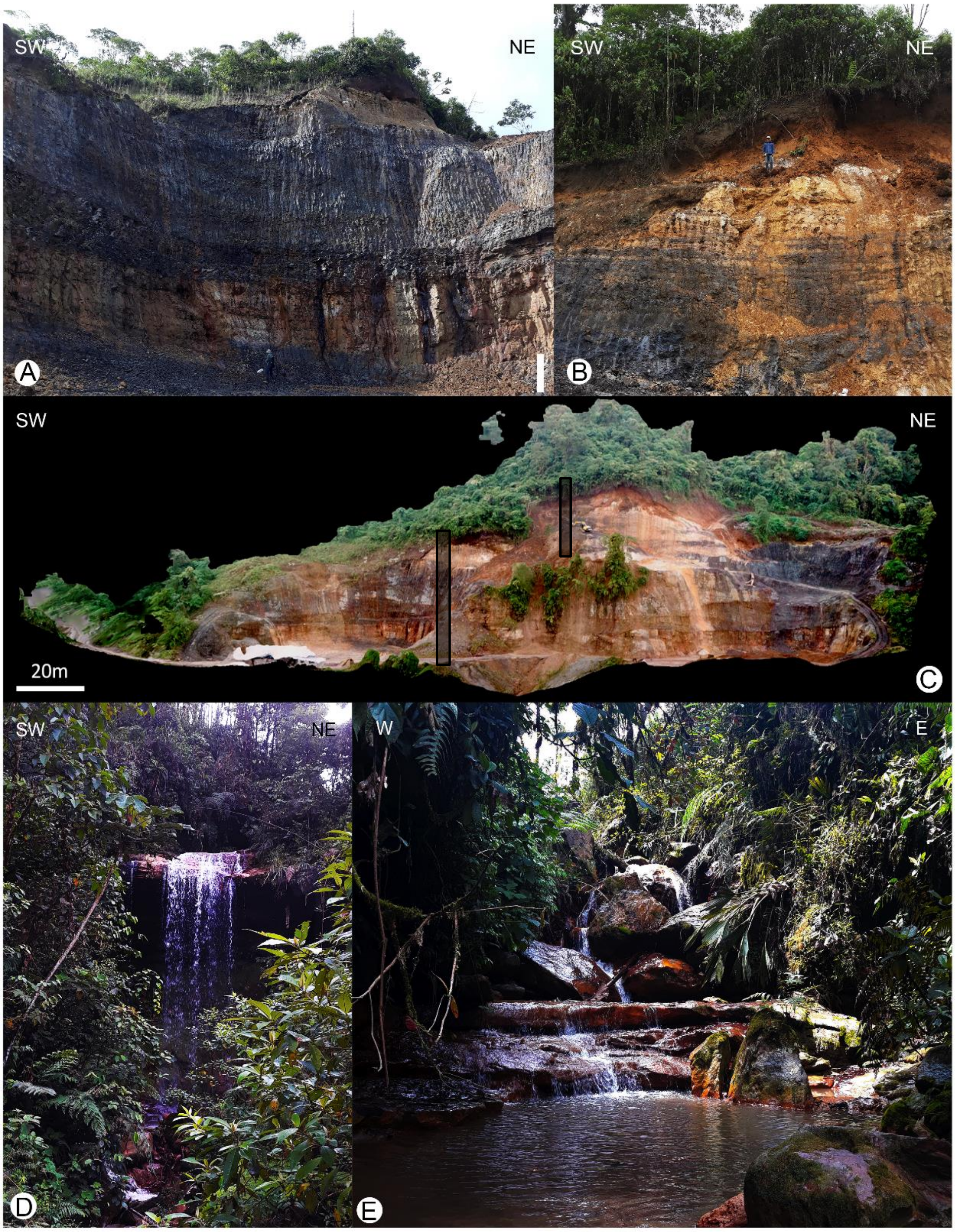

Figure 7. Genoveva Mine outcrops. Location 0°42'42.73"S, 77°47'17.83"W. A) First exploitation front in the Genoveva Mine. Scale bar 2 meters B) Top of Genoveva Mine. Men Scale 1.75 meters. C) Digital Elevation Model of Genoveva Mine constructed by Mauricio Baquero and Rafael Castaño. The shaded area represents the location of the stratigraphic column. D) Waterfall under of Genoveva Mine, 20 meters down the Hollin subsidiary river (0°42'40"S, 77°47'10 "W). E) Ravine located 0°42'41"S, 77°47'13 "W above the waterfall at 300 meters from first front of Genoveva Mine.

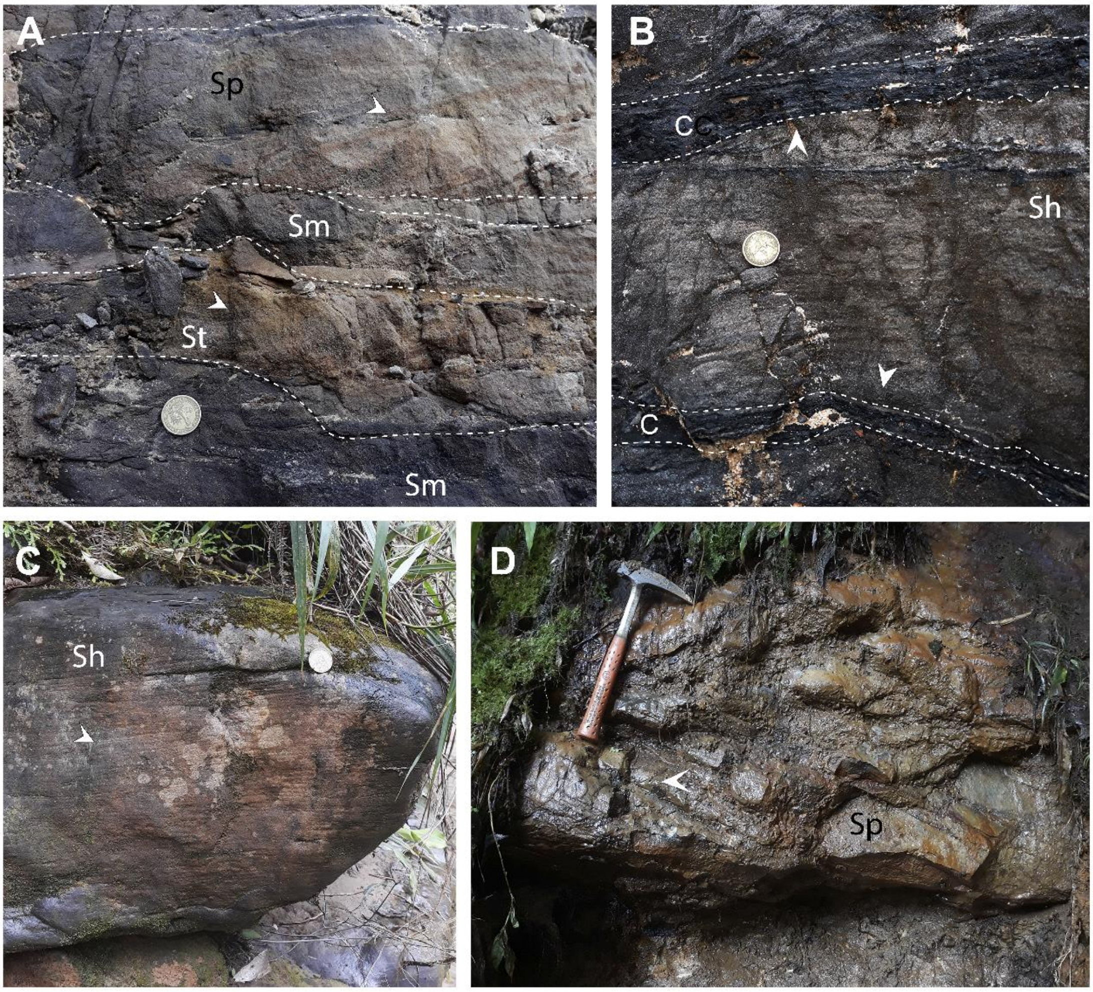

Figure 8. Lithofacies present in the lower part of the stratigraphic log at the Genoveva Mine. White arrows show sedimentary structures and coal layers. A) *Sm*, *St*, *Sp* lithofacies of active front of Genoveva Mine. B) Centimetric coal layers, *Sh* lithofacies from the active front of Genoveva Mine. C) *Sh* lithofacies at the ravine. D) *Sp* lithofacies at the top of waterfall. Coin diameter 26 mm. Hammer length 32,5 cm.

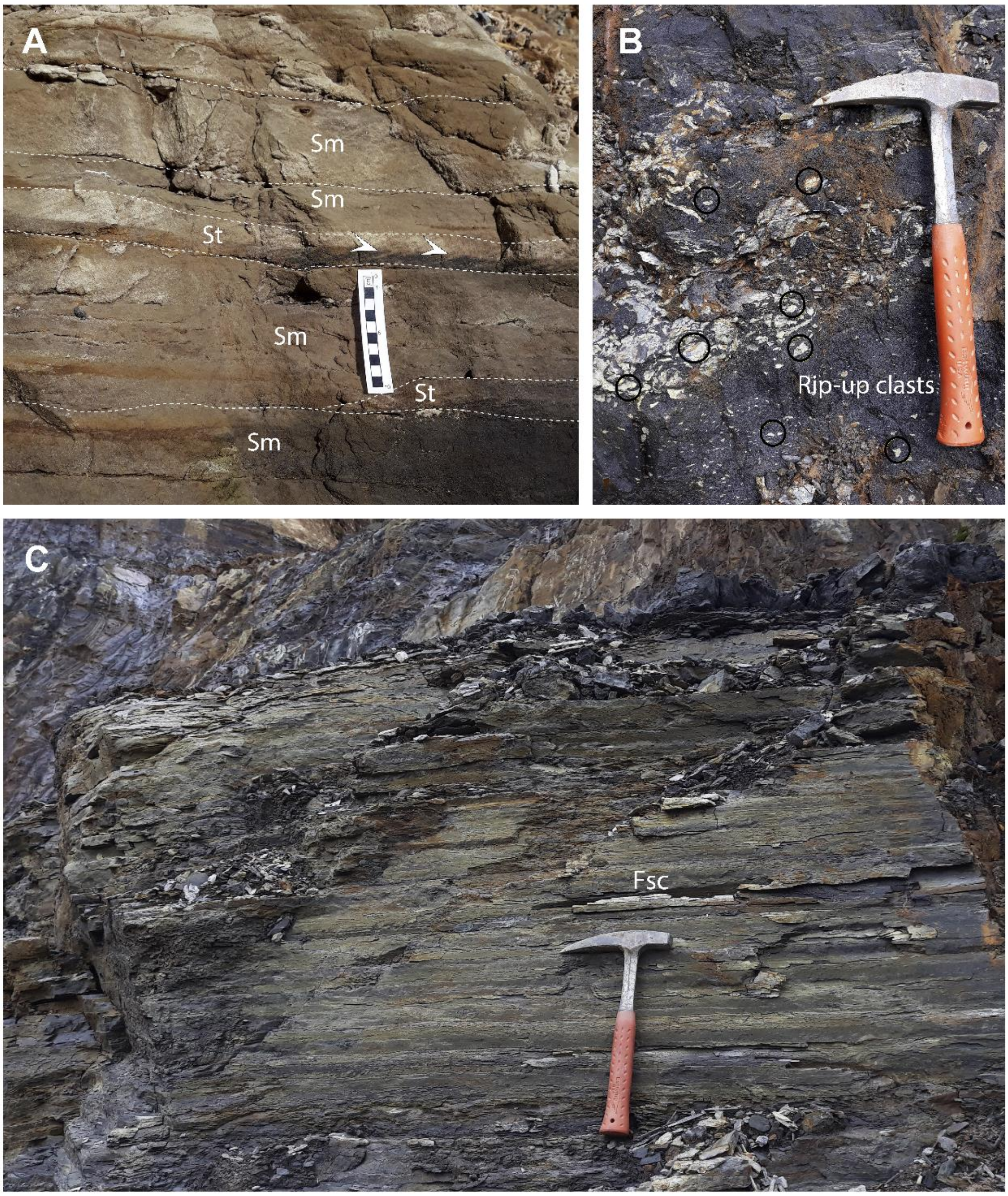

Figure 9. Lithofacies present in the middle part of the active front of Genoveva Mine. A) *Sm, St* lithofacies. White arrows show through cross-bedding structures. Scale bar 10 cm. B) Randomly distributed 1-50 mm rip-up silty clasts. C) *Fsc* lithofacies. Hammer length 32,5cm.

Table 3. Lithofacies and sedimentary structures, and depositional sub-environments identified at the middle part of the active Genoveva Mine employing the Miall (1978) code.

Lithofacies	***Description***	***Amber***	***Plant remains***	***Coal & organic debris***	***Bed Numbers***	***Sedimentary facies***
Fsc, *C*	Parallel-laminated fining upward very fine to silt siltstone; coal layers; parallel-laminated claystone.	X	X	X	36	Outer Lake
Fsc	Parallel-laminated siltstone with concretions and ripple laminations.		X		37	Middle – Outer Lake
Fsc, *Sp*, *Sh*, *Sm*	Parallel-laminated siltstone; planar cross-stratified fine sandstone; horizontal-laminated fine sandstone; massive medium sandstone.				16,56,57,58,59,60	Inner Lake
Fsc	Parallel-laminated siltstone with current ripples.				38	Bay
Sm	Medium to fine massive sandstone with silty rip-up clasts.				39,40,41,42,48,49,50	Hyperpycnal Flow
Sh, *Sm*, *Sp*	Parallel-laminated fine sandstone; massive fine to medium sandstone; planar cross-stratified fine to coarse sandstone.				14,15,17,20,43,61,62,63 64	Fluvial Bar
Fl	Parallel laminated siltstones and claystone.				65,70,72	Overbank
Fsc, *Sm*, *Sh*, *C*	Parallel-laminated siltstone with coal layers and organic remains; medium to fine massive sandstone; parallel-laminated medium sandstone with concretions.		X	X	44,45,46,47,51,52,53, 54,55,68,69,73	Fluvial Plain
Fsc	Parallel-laminated siltstone.				10	Interfluvial Channel
Sp, *Fsc*, *St*, *Sh*, *Sm*, *Sr*, *C*	Very coarse to fine planar cross-stratified sandstone; parallel-laminated very fine siltstone; through cross-bedded very coarse to fine sandstone; horizontal-laminated fine to coarse sandstone; massive very coarse to medium sandstone; massive sandstone with current ripples. Bed number 21 includes centimetrical clasts of amber and coal layers	X		X	3,4,5,6,7,8,9,11,13,18, 19,21,22,23,24,25,26, 27,28,29,30,31,32,33, 34,35,66,67,71	Fluvial Channel
Pl, *Pf*	Moderately consolidated paleosoil; pyroclastic flows with no apparent sedimentary structures.				1,2	Tuff

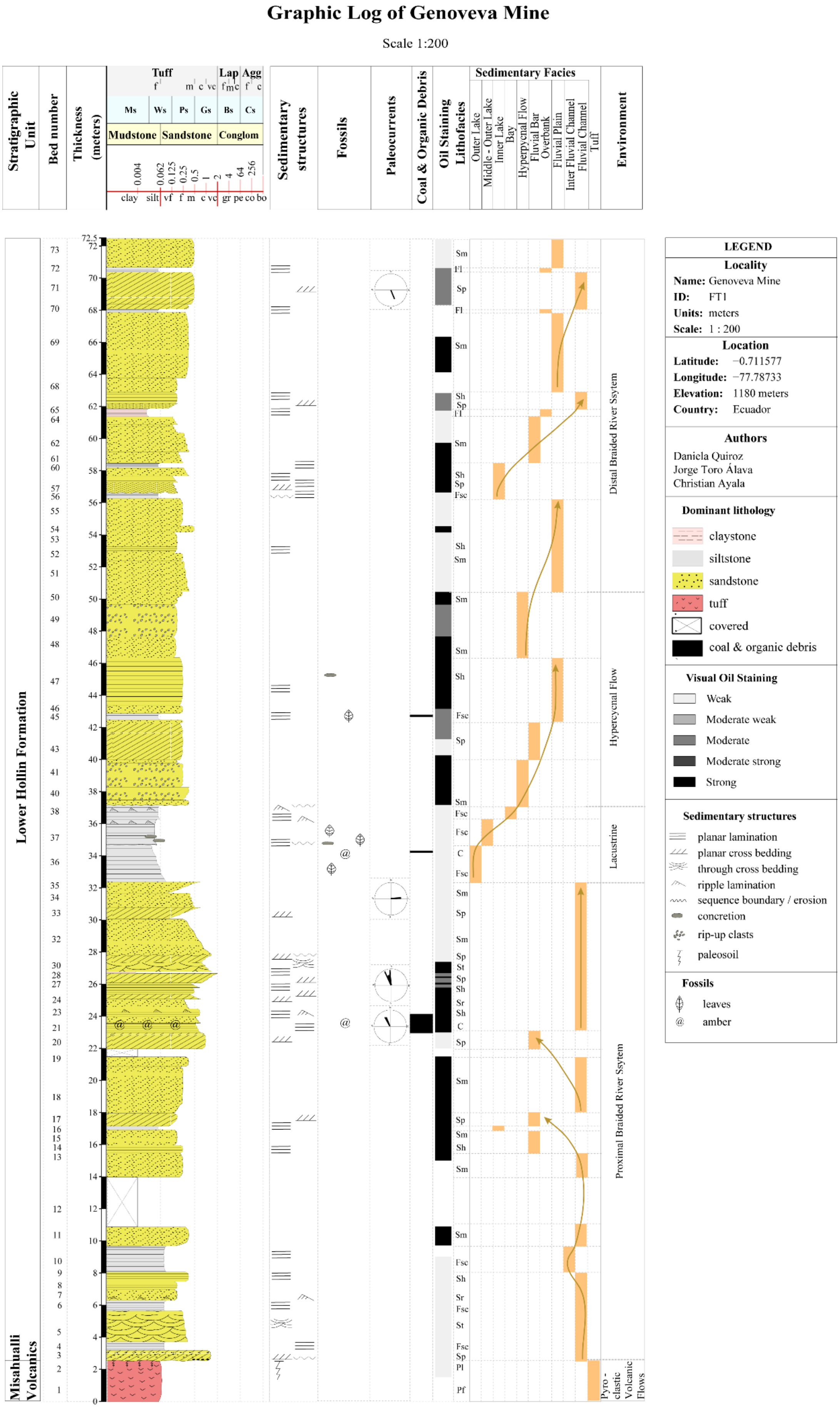

Figure 10. Stratigraphic Log of Genoveva Mine. See detail in Annex 2.

5.1.3 Abandoned Genoveva Mine

The stratigraphic log was described in one section from the abandoned exploitation front of Genoveva Mine (Figure 11). The stratigraphic column reached a total height of 15 meters (Figure 13). Four lithofacies and five depositional sub-environments were defined (Table 4). The identified lithofacies were: Horizontally-bedded sand (*Sh*); Massive sand (*Sm* - Figure 12B); Horizontally laminated to massive siltstone, silty claystone or claystone, (*Fsc* - Figure 12A), and Coal (*C* - Figure 12C).

Abundant plant macrofossils were recovered in the siltstone levels (see chapter 5.2.2) and three important coal layers (Figure 13).

Five depositional sub-environments were identified, from deepest to shallowest: Outer lake, Inner lake, Delta Lobe, Delta Plain, and Fluvial Channel.

Major environments identified in the Old Genoveva Mine, from deepest to shallowest, were: Lake, Delta, and distal Braided Stream River.

Figure 11. Outcrop of abandoned Genoveva Mine. The shaded area represents the location of stratigraphic column (0°42'42.920"S, 77°47'27.353"W).

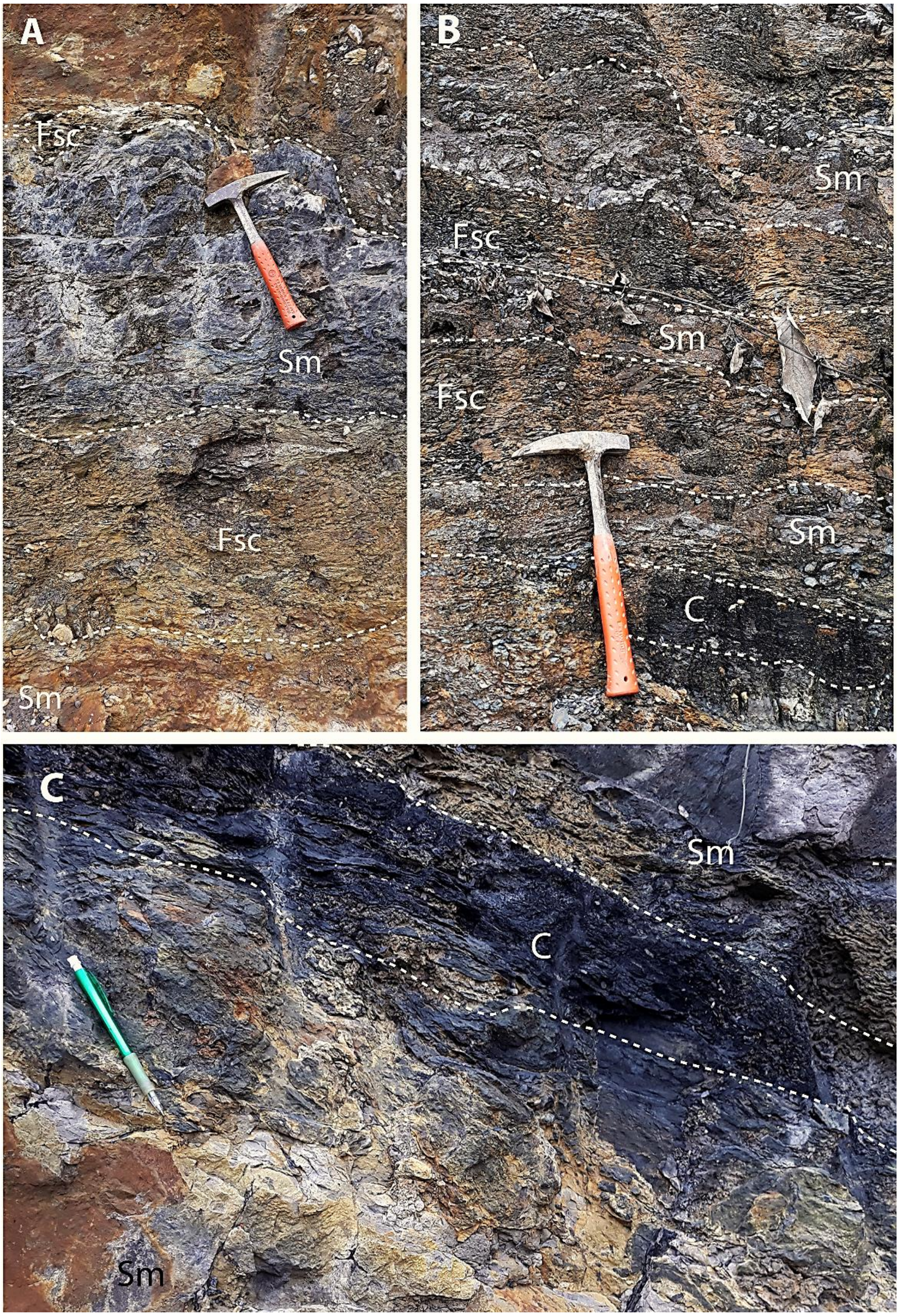

Figure 12. Lithofacies present in the abandoned front of the abandoned Genoveva Mine. A) *Sm*, *Fsc* lithofacies. B) Interbedded *Sm*, *Fsc & C* lithofacies. C) *Sm* and *C* lithofacies. Scales: hammer is 32,5 cm long, and pencil is 14 cm long.

Table 4. Lithofacies and sedimentary structures and depositional sub-environments identified at the middle part of the active Genoveva Mine employing the Miall’s (1978) code.

Lithofacies	***Description***	***Amber***	***Plant remains***	***Coal & Organic debris***	***Bed Numbers***	***Sedimentary Facies***
Fsc, Sm	Parallel-laminated siltstone; massive very fine sandstone				19,20,21, 22,23	Outer Lake
Fsc, Sh	Parallel-laminated siltstone with plant remains; Parallel-laminated very fine sandstone with amber clasts.	X	X		1,2,3,25,26	Inner – Outer Lake
Fsc	Massive very fine siltstone, parallel-laminated siltstone.		X		8,15	Inner Lake
Fsc, Sm, C	Massive siltstone; massive fine to very fine sandstone; coal layers.		X	X	9,10,11,12, 13,14	Delta Plain-Inner Lake
Sh	Parallel-laminated fine sandstone.				24	Delta Lobe
Sm, C	Massive very fine sandstone; coal layer.		X	X	16,17,18	Delta Plain – Delta Front
Sm, Fsc, Sh	Massive fine sandstone; massive siltstone; Parallel-laminated very fine sandstone.		X		4,5,6,7	Fluvial Channel

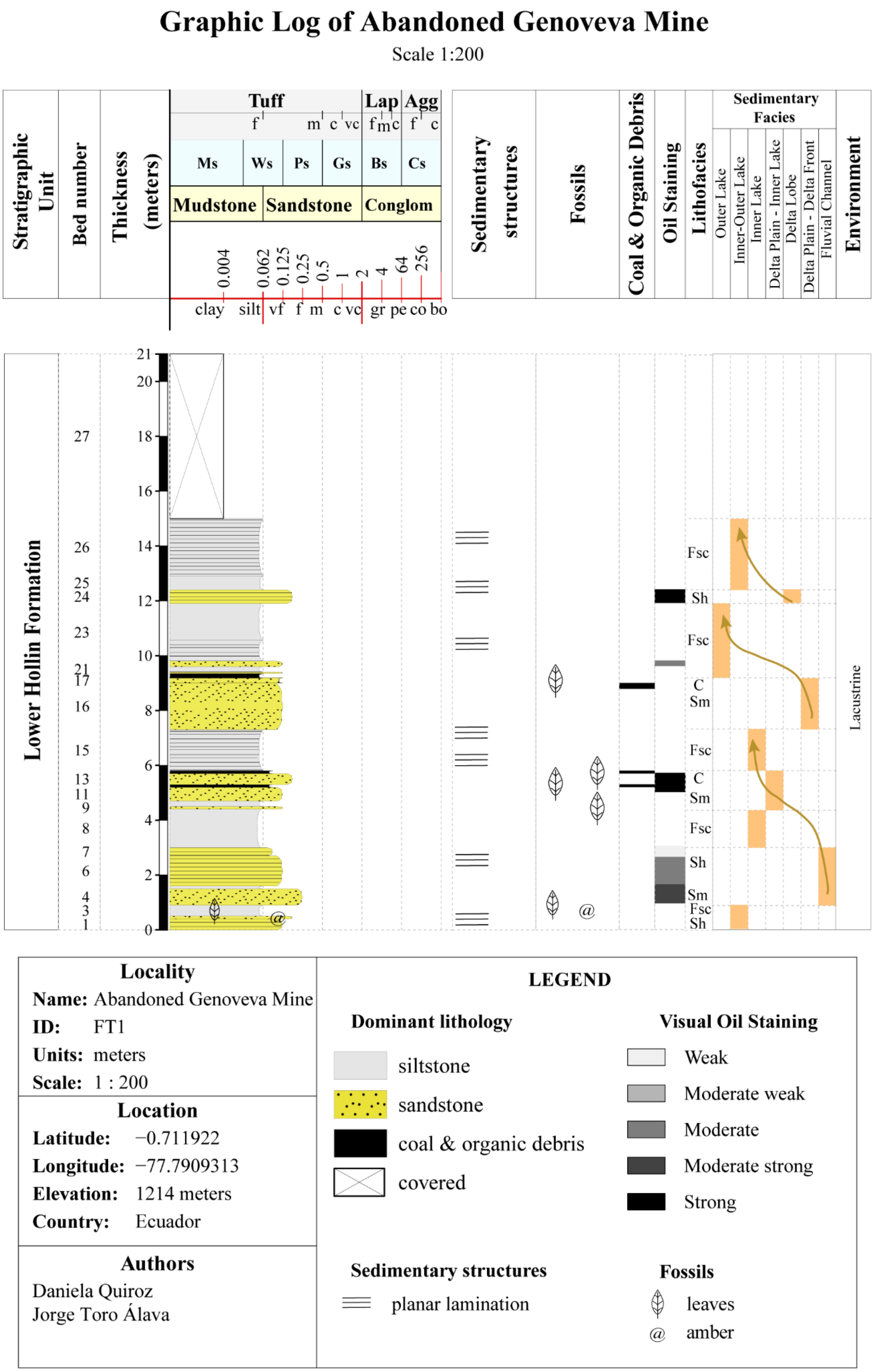

Figure 13. Stratigraphic Log of abandoned Genoveva Mine. See details in Annex 3.

5.2 Paleobotanic Results

5.2.1 Fossil Cuticles

Clastic rock samples containing fossil cuticles were collected from two localities in the Pungarayacu area at a distance of ~250 meters between them. The first collection (Figure 14) was done in 2018 by Dr. Edwin Cadena; however, the exact location could not be found since the stratigraphic log is missing. The second collection (Figure 15) was carried out during the field trips of this research project; thus, the precise location is known (see the graphic log of Figure 6).

Twenty-five slides were prepared, which contain 10 – 20 cuticle samples per slide. In total, seven morphotypes were identified. The description method is based on Peppe et al., 2008. The cuticle position, either abaxial or adaxial, is unknown.

HF01

Figure 14A & Figure 15A

"Cupressaceae"

Systematic affinity:

Class Pinopsida

Order Pinales

Family Cupressaceae

Description: Epidermal fragment with rectangular epidermal cells 37 µm - 77 µm long, 8 µm – 12 µm wide (Figure 14A). The fragment exhibits lateral stomatal bands parallel oriented to epidermal cells. Each band is generally about one stoma wide. The stomatal complex is tetracytic formed by two polar cells and two or three lateral cells. Guard cells are absent. Each stoma is 41 µm - 58 µm long, 55 µm – 72 µm wide (Figure 14A). The fragment has abundant epicuticular wax crystals distributed over the epidermal cells (Figure 15A).

Morphotype exemplar. HF01

HF02

Figure 14B

Systematic affinity: Unknown. Probable angiosperm

Description: The epidermal pattern is unknown. This morphotype exhibits the stomata complex in detail, two guard cells and the pore, and an apparent single subsidiary cell. However, other subsidiary cells can be sunkenly surrounding the guard cells. Thus, the stomatal complex, 88 µm long, 77 µm wide, can be anysocytic.

Morphotype exemplar. HF02

HF03

Figure 14C

Systematic affinity: Unknown. Probable angiosperm

Description: Epidermal leaf fragment with well-defined symmetrical and asymmetrical cells, 42 µm long and 40 µm wide, does not follow any orientation. The stomata are sunken and present well-developed guard cells and cuticular striations radiating from guard cells. Subsidiary cells are absent. The anomocytic stomata measure 39 µm - 47 µm long, 20 µm – 30 µm wide.

Morphotype exemplar. HF03

HF04

Figure 14D

"Ring"

Systematic affinity: Unknown

Description: Leaf fragment composed of four stomatal bands 112 µm – 224 µm wide. Each band is generally about two to four stomata wide. The epidermal cells are not well defined but have an elongated shape. The stomata measure 4 µm - 5 µm wide and 7 µm – 10 µm long. The guard cells are absent. Five to seven subsidiary cells form a ring around the stomatal aperture.

Morphotype exemplar. HF04

HF05

Figure 14E

"Podocarpaceae"

Systematic affinity:

Class Pinopsida

Order Araucariales

Family Podocarpaceae

Description: Leaf fragment with rectangular and elongated epidermal cells, 54 µm - 97 µm long, 18 µm – 24 µm wide parallel to each other. The stomata are randomly placed over the fragment but longitudinally oriented with epidermal cells. The stomata measure 37 µm - 40 µm long, 28 µm - 36 µm wide. The guard cells are well-defined, shorter than epidermal cells. The subsidiary cells are absent.

Morphotype exemplar. HF05

HF06

Figure 14F

Systematic affinity: Unknown

Description: Leaf epidermis with notably elongated cells that vary from trapezoidal to rectangular. They measure 112 µm – 121 µm long and 10 µm - 17 µm wide. The stomata are parallel oriented to the epidermal cells, 32 µm – 35 µm long and 15 µm - 16 µm wide. Subsidiary cells are poorly defined, and the stomata are paracytic, seemingly sunken into the epidermis.

Morphotype exemplar. HF06

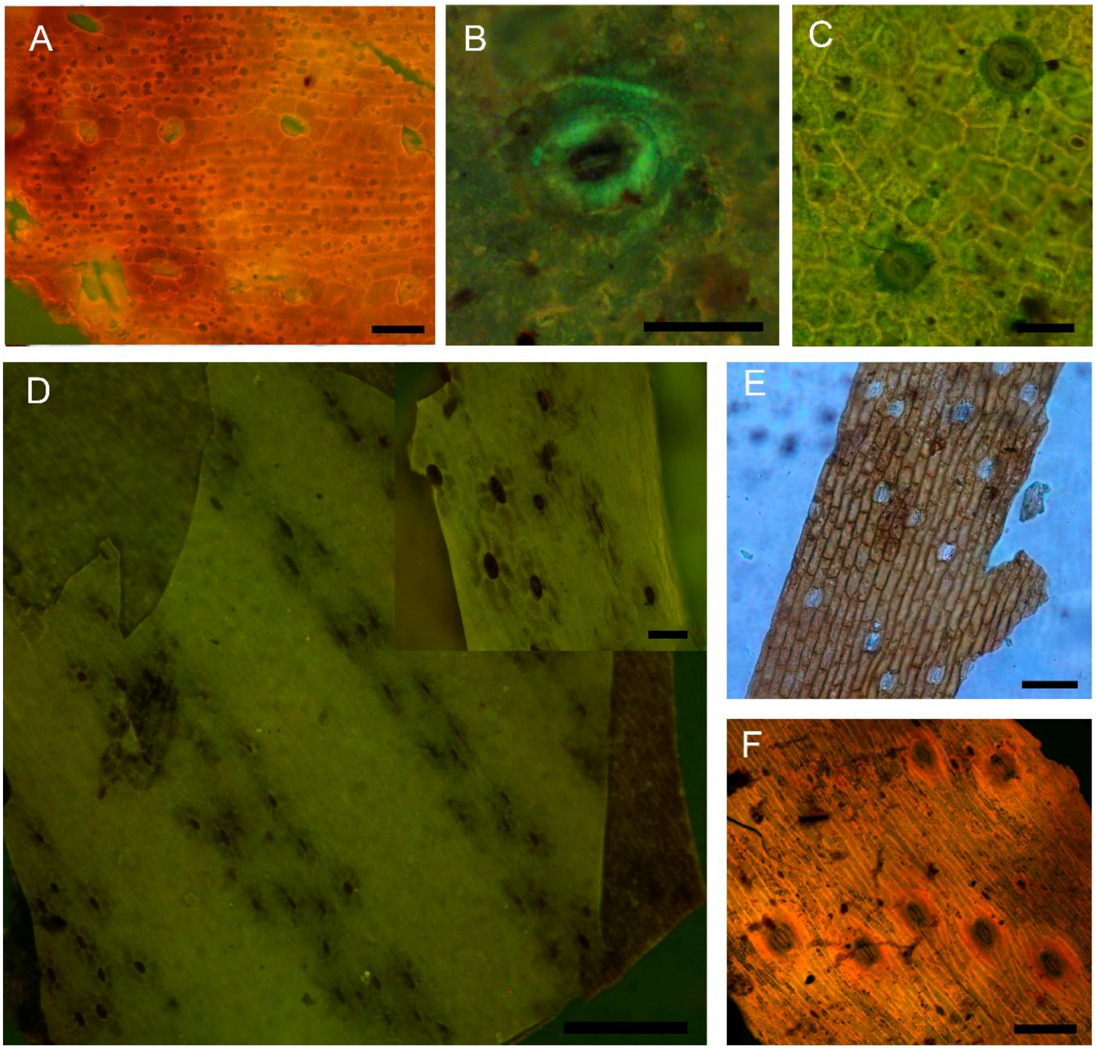

Figure 14. Fossil cuticle fragments from the first collection of Pungarayacu Quarry. (A) HF01 morphotype exhibit the stomatal bands. Scale bar 50 µm. (B) HF02 morphotype showing the guard cells, the stomata aperture, and a single subsidiary cell. Scale bar 50 µm. (C) HF03 morphotype showing well-preserved guard cells and epidermal cells. Scale bar 50 µm. (D) HF04 morphotype evidencing stomatal bands formed by two to four stomata. Scale bar 100 µm. Rings of subsidiary cells are located around the stomata aperture where guard cells are absent. Scale bar 50 µm within the inception. (E) HF05 morphotype presents rectangular epidermal cells with well-preserved guard cells. Scale bar 100 µm. (F) HF06 morphotype showing elongated epidermal cells and well-preserved guard cells. Scale bar 100 µm. Photographs were taken with Olympus DP73/BX63 Microscope and epifluorescence Nikon Eclipse E600 Microscope.

HF07

Figure 15B

Systematic affinity: Unknown

Description: Cuticle fragment with not well-defined epidermal cells. The stomata are randomly distributed, 117 µm – 135 µm long and 89 µm – 132 µm wide.

The guard cells are conspicuous, but the subsidiary cells are not well defined or are apparently absent. A thin ring surrounds the stomata complex.

Morphotype exemplar. HF07

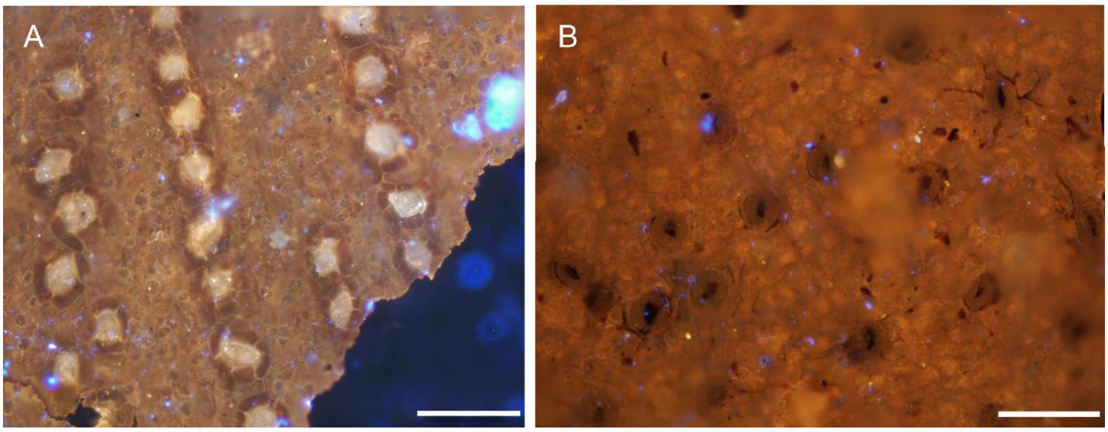

Figure 15. Fossil cuticle fragments from the second collection of Pungarayacu outcrop. A) HF01 morphotype exhibit the stomatal bands. Scale bar 200 µm. (B) HF07 morphotype showing the guard cells, the stomata aperture, and a single subsidiary cell. Scale bar 300 µm. Photographs were taken with epifluorescence Olympus DP73/BX63 Microscope.

5.2.2 Leaf macrofossils

The leaf macrofossils were mainly collected in two places, at the Genoveva Mine and the abandoned Genoveva Mine during the second field trip organized by Dr. Carlos Jaramillo and Dr. Fabiany Herrera researchers from the Smithsonian Tropical Research Institute and the Chicago Botanic Garden, respectively. The fossils are well-preserved in fine-grained siltstones. Foliar margins and venation patterns of the leaves are preserved in most of the specimens collected. Fifteen leaf morphotypes were identified.

Morphotype **HF 08**

Class Cycadopsida

Order Cycadales

Leaves are elongated, narrow, entire margined, bases and apices are not preserved (Figure 16). The specimen measures on average 3 cm long and 1 cm wide. The main characteristic is the parallel venation, with 20-30 veins.

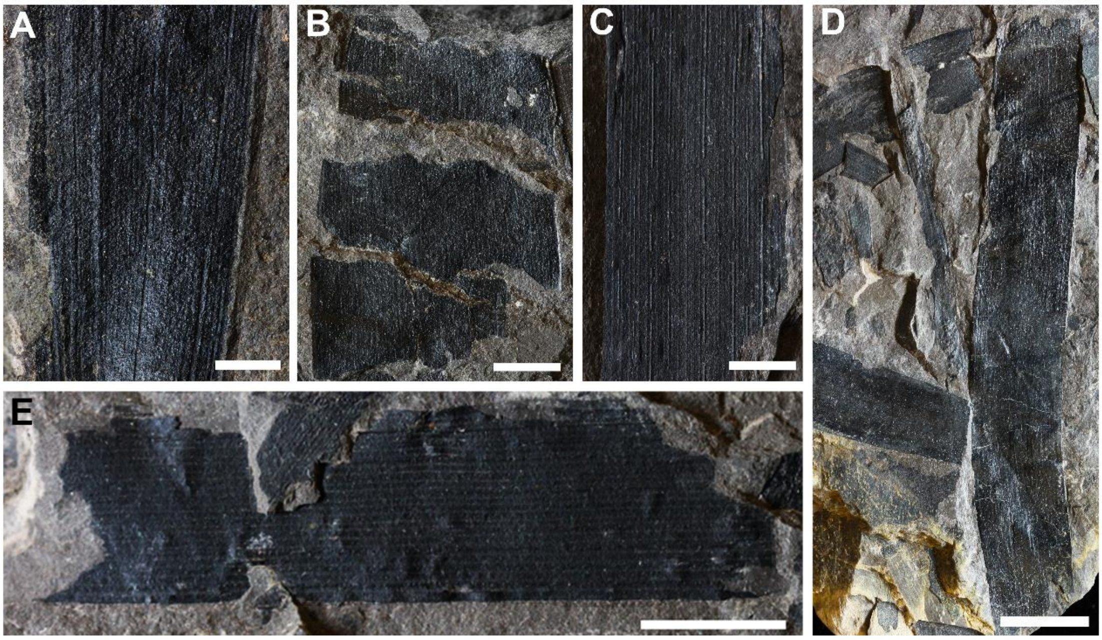

Figure 16. Probably Cycad leaf fragments. A) Scale bar 5 mm. Length 28 mm and wide 17mm. B) Scale bar 5 mm. Length 27 mm and wide 18 mm. C) Scale bar 5 mm. Length 27 mm and wide 13 mm. D) Scale bar 5 mm. Length 34 mm and wide 5 mm. E) Scale bar 10 mm. Length 51 mm and wide 13 mm.

Morphotype **HF 09**

Order Coniferales

Family Cupressaceae

Carbonized leaves with an alternate position of foliage branches in a plane. The angles between the primary branch and secondary branches are 40º - 45º (Figure 17D - Figure 17E). The branch leaves are decussate, scale-like, imbricate, and entire margined. The base is decurrent and the apex is acute. The branches are, on average, 16 mm long and 2 mm wide (Figure 17A-C).

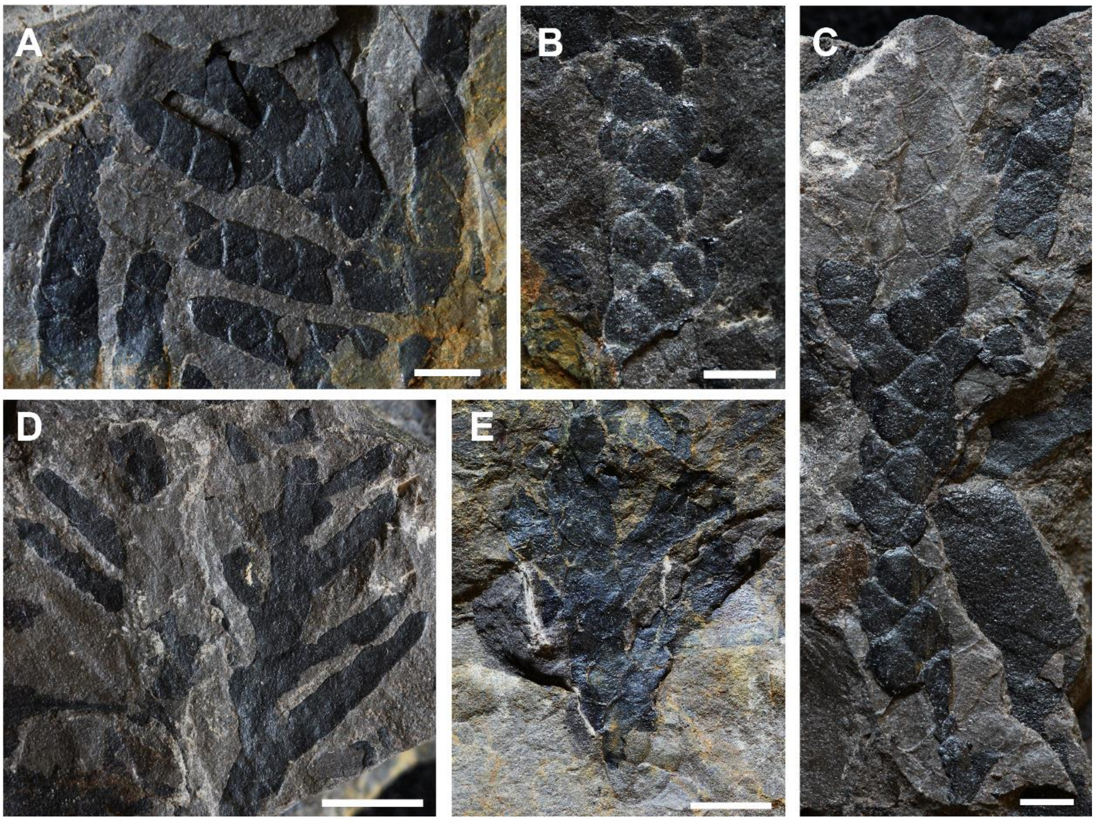

Figure 17. Conifer leaves fragments. A) Scale bar 2 mm. Length 10 mm and wide 1-2 mm. B) Scale bar 2 mm. Length 12 mm and wide 3 mm. C) Scale bar 2 mm. Length 27 mm and wide 3 mm. D) Scale bar 5 mm. Length 23 mm and wide 3 mm. E) Scale bar 5 mm. Length 22 mm and wide 2-3 mm.

Morphotype **HF 10**

Order Coniferales

Family Cupressaceae

Fragments of vegetated shoots with flattened leaves, slender, falcon-shaped, decussate, scale-like, entire margined, decurrent, with an acute apex, born in pairs with an opposite arrangement. Lateral leaves diverge from the axes at acute angles from 39º to 41º (Figure 18A). Central leaves are rhombic with circular leaves above each one.

Morphotype **HF 11**

Order Coniferales

Family Cupressaceae

Lateral leaves 11mm long and 3 mm wide, straight upward, entire margin, decurrent, with a rounded apex, born in pairs with an opposite disposition (Figure 18B). They evidence a mid-vein. Short-space rings form the central stem.

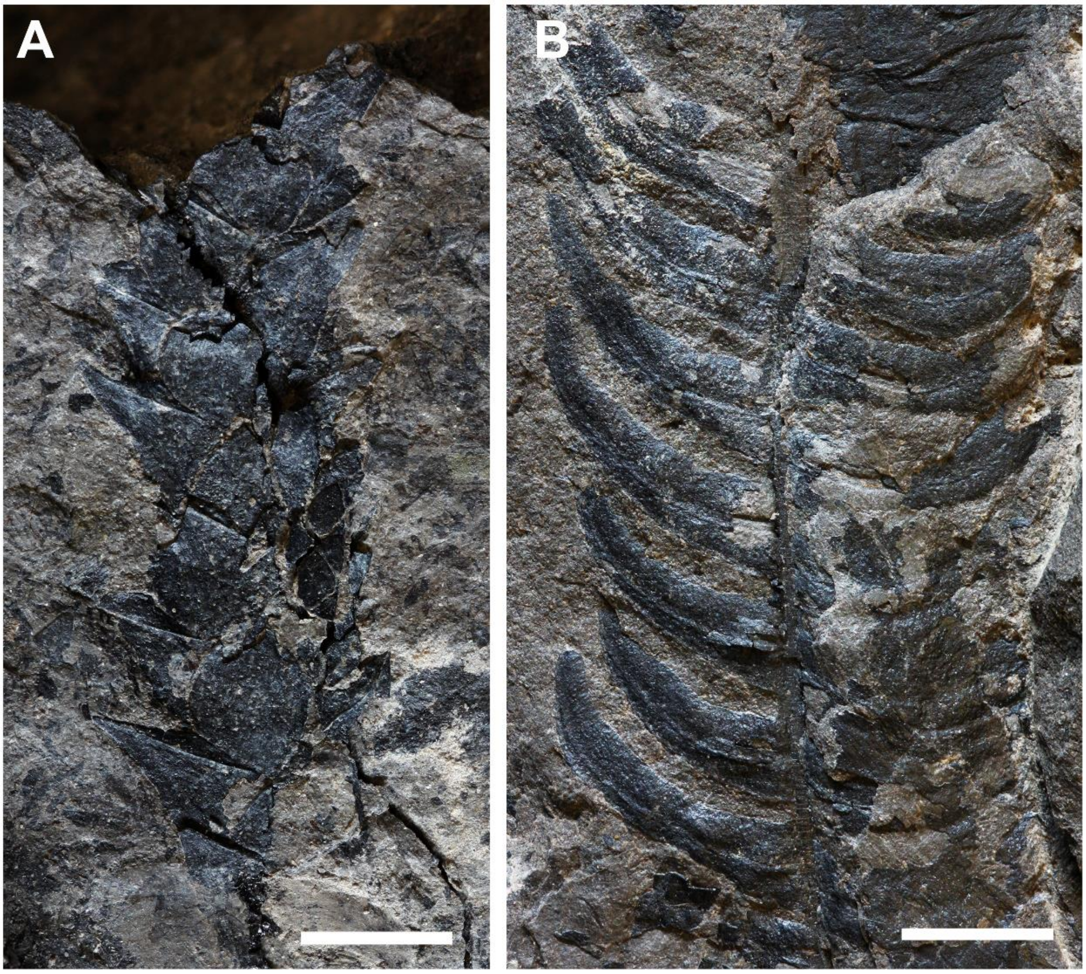

Figure 18. Conifer leaves fragments. A) Scale bar 5 mm. 27 mm long and 9 mm wide. B) Scale bar 5 mm. 28 mm long and 16 mm wide.

Morphotype **HF 12**

Family Podocarpaceae

Leaves are narrowly oblong to strap-shaped, bilaterally symmetrical, with entire margins. The base is cuneate, and the apex is lanceolate (Figure 19D). The widest part of the leaf is in the middle. On average, the leaves measure 20-55 mm long and 17-20 mm wide. There are conspicuous, 10-50 longitudinal veins that arise from the leaf base to the apex. They are parallel and evenly distributed along with the leaf (Figure 19A-C).

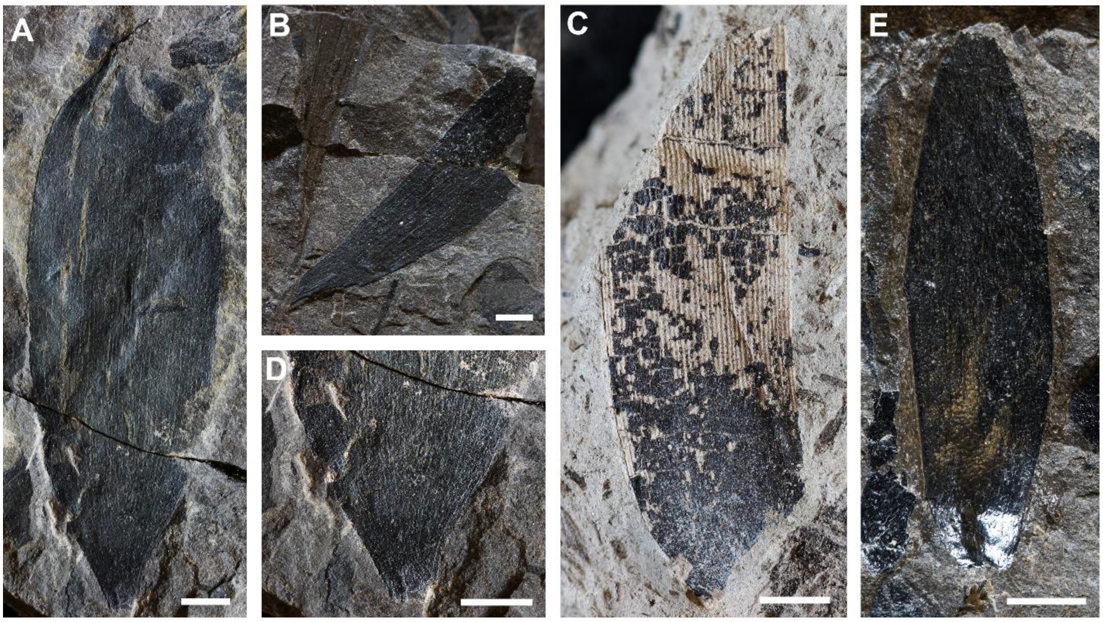

Figure 19. Conifer leaves fragments. A) Scale bar 5 mm. Length 57 mm and wide 19 mm. B) Scale bar 2 mm. Length 18 mm and wide 5 mm. C) Scale bar 5 mm. Length 43 mm and wide 13 mm. D) Scale bar 3 mm. Length 12 mm and wide 11 mm. E) Scale bar 5 mm. Length 33 mm and wide 9 mm.

Morphotype **HF13**

Fern I

Systematic Affinity: Unknown

Frond fragments (Figure 20A - B). Short pinnules (2 mm long and 1 mm wide), acute apex, decurrent base, straight upward, entire margin, mid-vein evidence, born in pair with an alternate disposition (Figure 20A). The pinnae are composed of pinnules joined to each other, forming a smooth sinuate margin (Figure 20B). The central stem and costa are well-preserved. The base of the pinnules is the widest part.

Morphotype **HF14**

Fern II

Systematic Affinity: Unknown

Pinna fragment. The pinnules are upward, alternated disposition, entire margined, sharp apex (Figure 20D) or lanceolate apex (Figure 20C) and decussate base slightly flared. There is a midvein from which detaches several upward smaller veins.

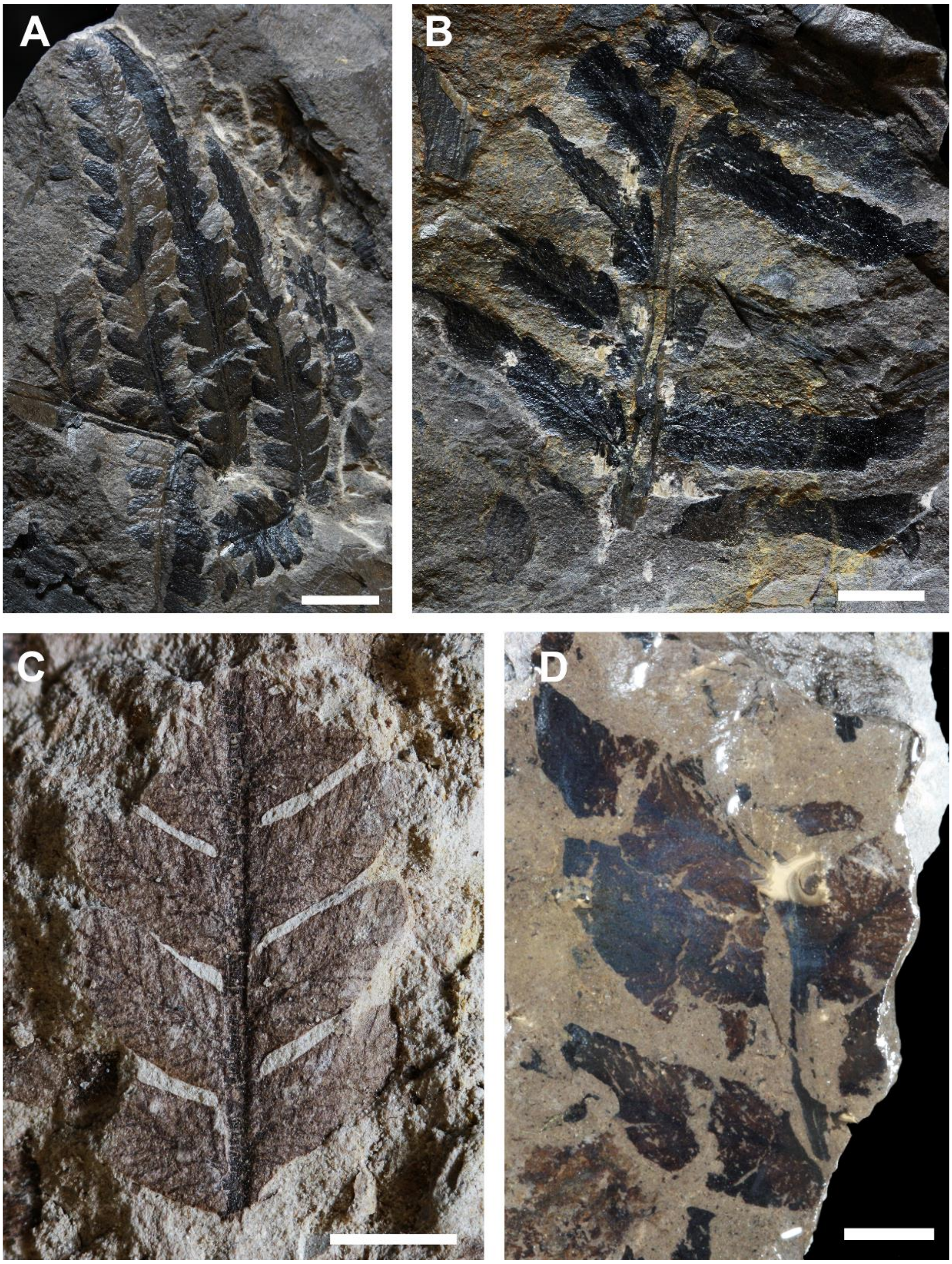

Figure 20. Fern leaves fragments. A) Scale bar 4 mm. Pinna length 30 mm and wide 3 mm. B) Scale bar 4mm. Pinnule length 12 mm and wide 3 mm. C) Scale bar 3 mm. Length 13 mm and wide 7 mm. D) Scale bar 3 mm. Length 9 mm and wide 3 mm

Morphotype **HF 15**

Fern III

Systematic Affinity: Unknown

Carbonized pinna fragment. The pinnules (Figure 21A) are entire margin, rounded apex, decussate, perpendicular oriented to the costa, close to each other with conspicuous mid-veins.

Morphotype **HF 16**

Fern IV

Systematic Affinity: Unknown

Ovate leaf, acute base (Figure 21B), spiny margin with the widest part at the leaf center (Figure 21B-C). The venation pattern is unclear.

Morphotype **HF17**

Fern V

Systematic Affinity: Unknown

Fan-shaped leaf fragment (Figure 21D). Acute base and absent apex. The mid-vein is prominent. Many secondary, closely spaced veins diverge from the midvein. Secondary veins diverge from 30º to 60º degrees.

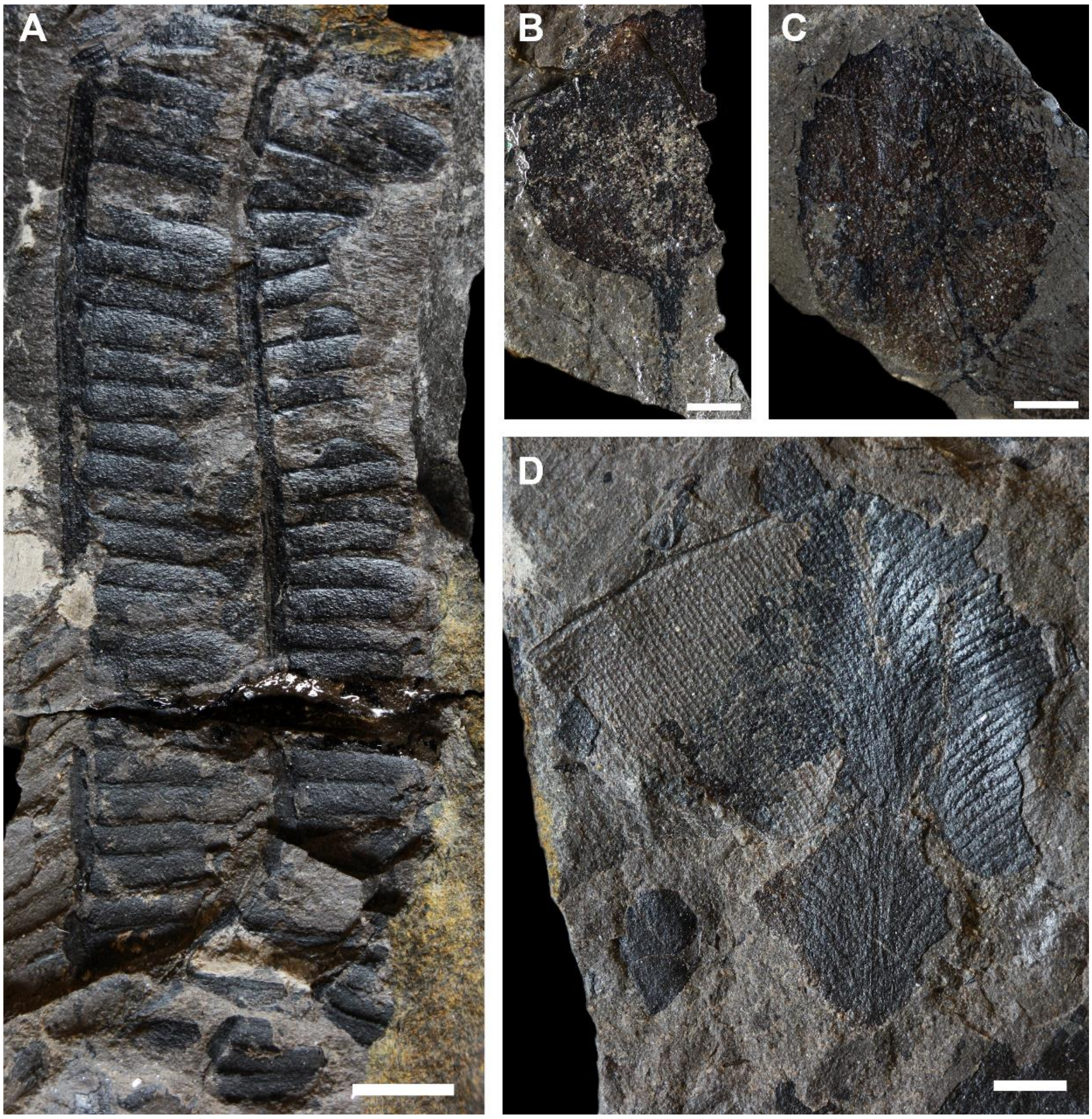

Figure 21. Fern leaves fragments. A) Scale bar 5 mm. Length 52 mm and wide 15 mm. B) Scale bar 3 mm. Length 15 mm and wide 11 mm. C) Scale bar 2 mm. Length 10 mm and wide 8 mm. D) Scale bar 2 mm. Length 15 mm and wide 14 mm.

Morphotype **HF 18**

Class Lycopodiopsida

Order Selaginellales

Family Selaginellaceae

Leafy fragment of 18 mm long and 4 mm wide. Leaves are short (2 mm long and 0.8 mm wide), upward, opposite disposition, entire margined, with a rounded apex and decussate base (Figure 22B). The leaves are overlapped with each other. Their midvein is unclear.

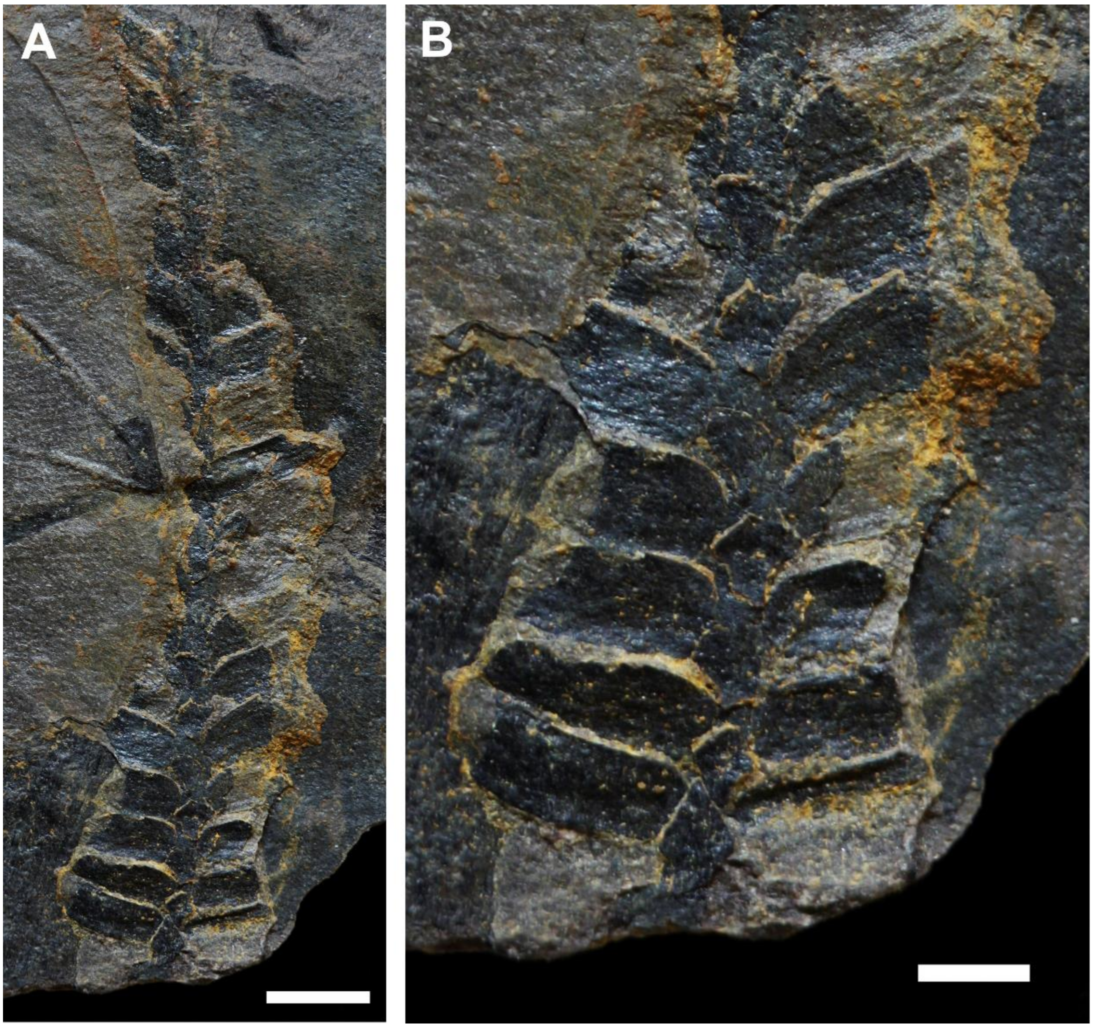

Figure 22. Leaf fragment. A) Scale bar 2 mm. Length 18 mm and wide 4 mm. B) Scale bar 1mm. Pinnules measure 2 mm long and 0.8 mm wide.

Morphotype **HF 19**

Angiosperm I

Systematic Affinity: Unknown

Leaf pinnate with a stout petiole and midvein. Leaf shape elliptic. Apex and base are approximately convex. Figure 23A shows a convex apex and base. Petiole ~9mm long and 3 mm wide. Leaf margin entire. Leaf size mesophyll, Figure 23A measures 56 mm long and 16 mm wide, whereas Figure 23B 38 mm long and 18 mm wide. The venation is not well-distinguished; however, there can be an apparent midvein and secondary venation in Figure 23B.

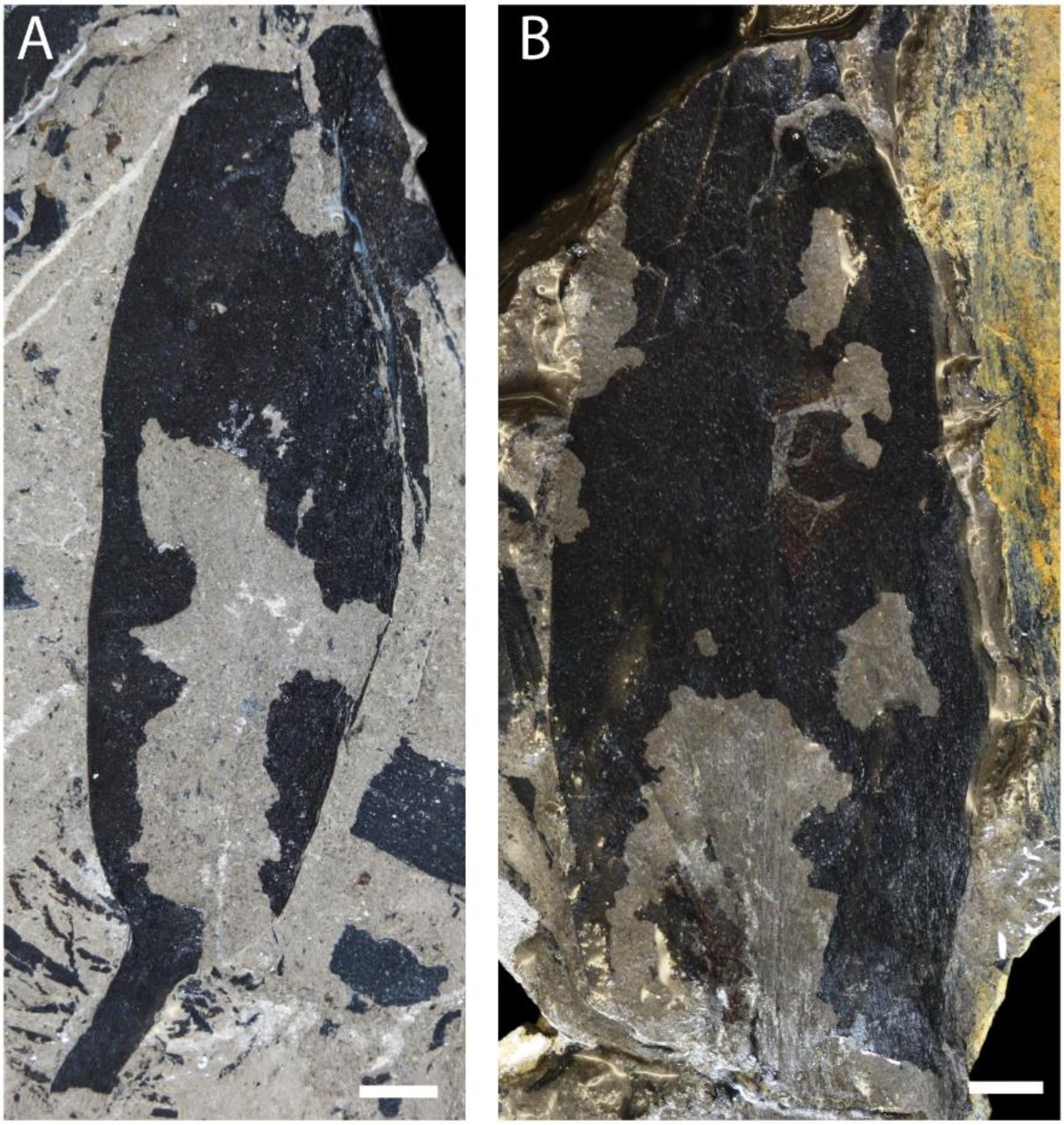

Figure 23. Possible angiosperm leaves. A) Scale bar 4 mm. Length 56 mm and wide 16 mm. B) Scale bar 3 mm. Length 38 mm and wide 18 mm.

Morphotype **HF 20**

Angiosperm II

Systematic Affinity: Unknown

Pinnate leaf. Midvein thin. Leaf shape elliptic. Leaf apex acuminate (without drip tip). Leaf margin entire. Secondary vein brochidodromus. Tertiary veins reticulate (Figure 24). Leaf size 30 mm long and 13 mm wide. The petiole and base are not preserved.

Morphotype **HF 21**

Angiosperm III

Systematic Affinity: Unknown

Pinnate leaf. Midvein thin. Leaf shape ovate. Base shape rounded. Apex shape acuminate (without drip tip). Leaf margin entire. Leaf size 22 mm long and 9 mm wide (Figure 25A).

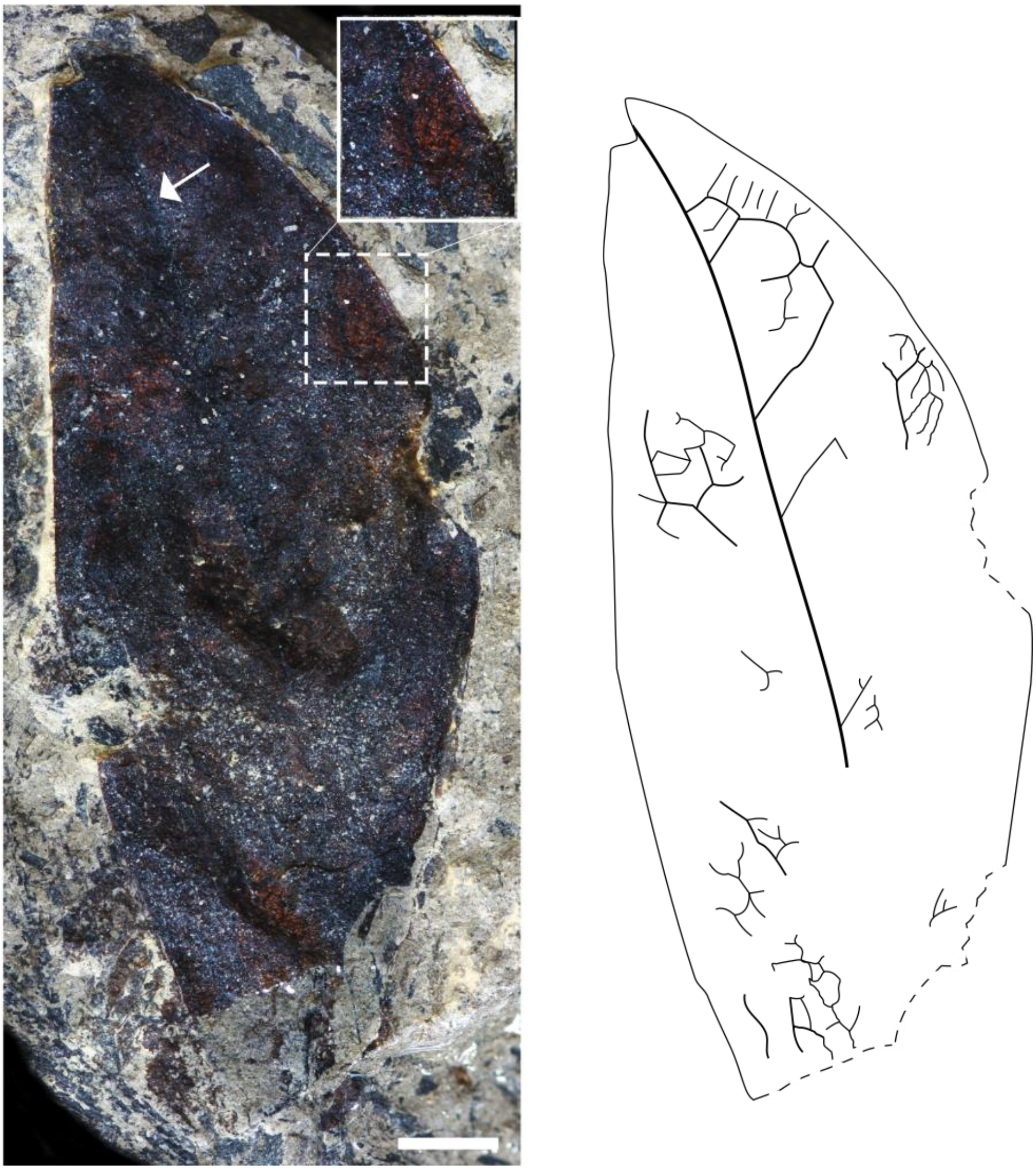

Figure 24. Possible angiosperm leaves. A) Scale bar 3 mm. Length 30 mm and wide 13 mm.

Morphotype **HF 22**

Angiosperm IV

Systematic Affinity: Unknown

Leaf fragment, likely actinodromus with cordate base (Figure 25B). Major secondary veins strongly festooned brochidodromous. Tertiary and quaternary veins looped. Leaf margin entire. Leaf size 14 mm long and 24 mm wide.

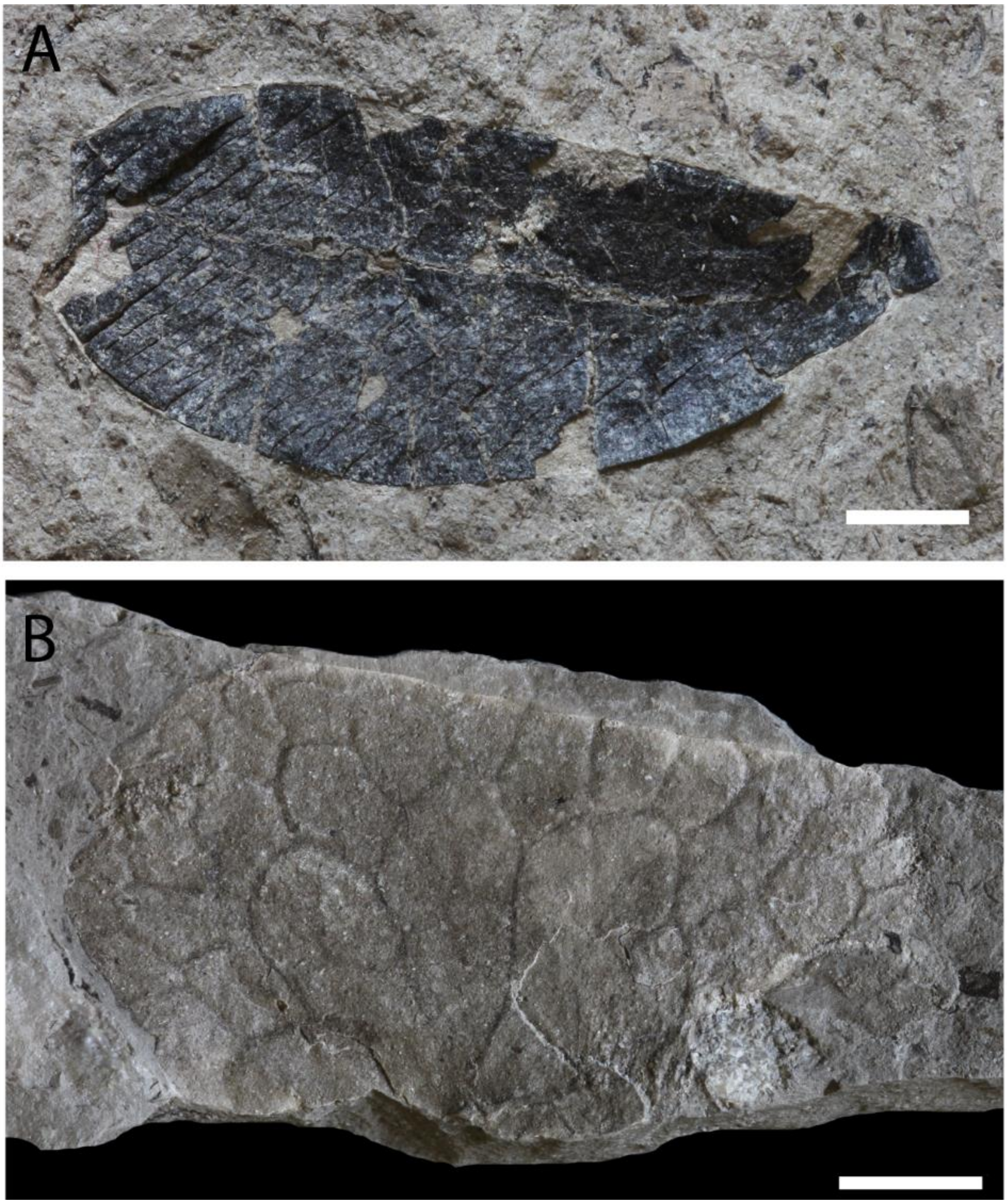

Figure 25. Possible angiosperm leaves. A) Scale bar 3 mm. Length 22 mm and wide 9 mm. B) Scale bar 4 mm. Length 14 mm and wide 24 mm.

5.2.3 Amber

Amber pieces and fragments were mainly found embedded in sandstones, although they were also observed in siltstones, where sandy fragments rest on laminations. They are commonly close to coalified layers. Amber fragments do not have a defined shape; however, they appear lenticularly shaped in most cases. Amber color is variable between brown-reddish, orange (Figure 26A), and yellow to green (Figure 26B).

More than 2000 amber samples from the Genoveva Mine were collected and inspected. No evidence of embedded organic remains was observed, such as flowers, cones, seeds, leaves, etc. The size of the amber samples varies from 1 to 30 cm and have microbubbles (Figure 27B), oil intrusions, and multiple conchoidal fractures (Figure 27C) that can be easily confused with organic remains.

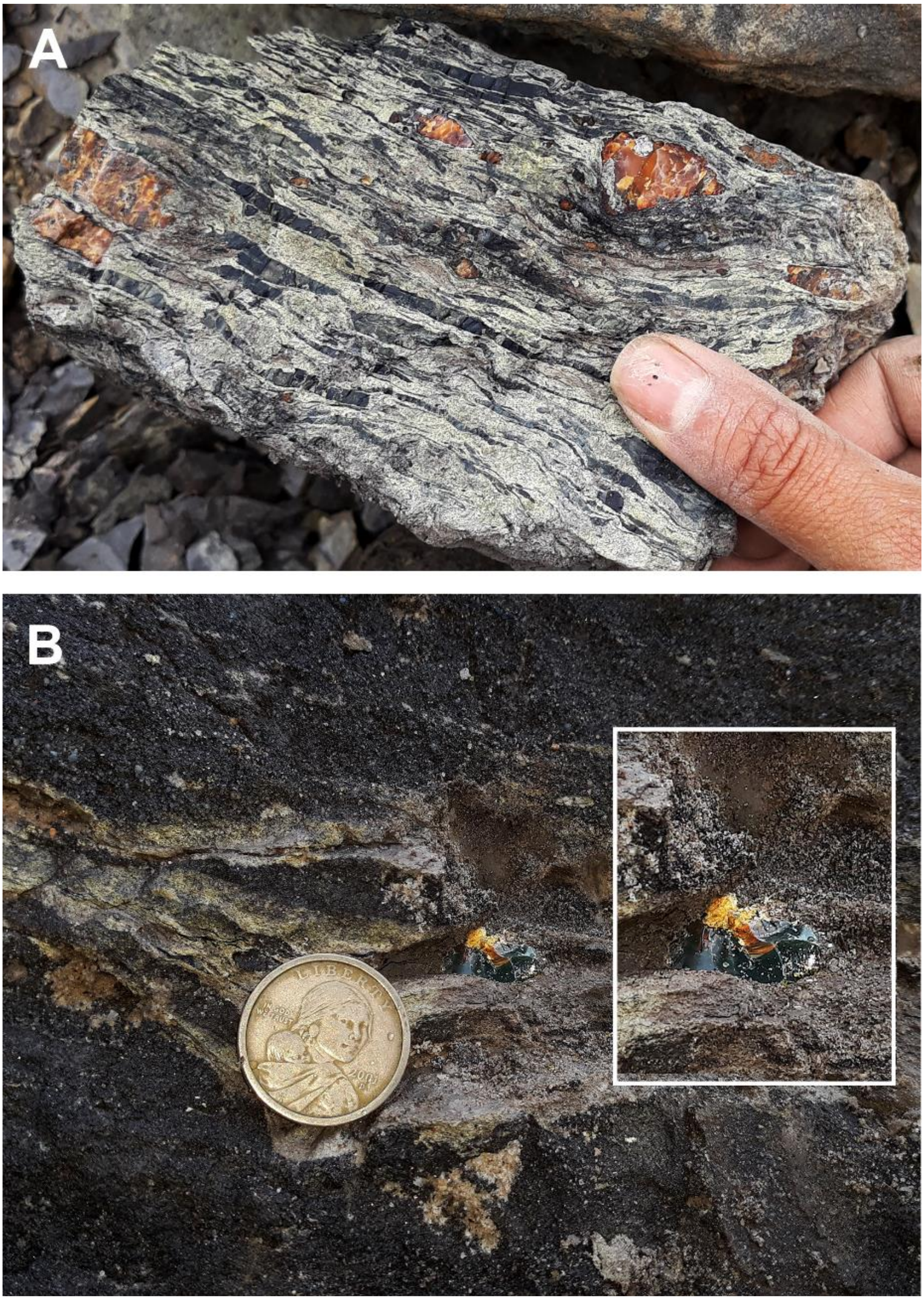

Figure 26. Amber fragments *in-situ*. A) Light gray fine sandstone interbedded with coal layers and amber pieces. Amber is embedded in the sandstone, orange in color, fragmented, and lenticular shaped. B) Oil-stained medium to coarse-grained sandstone interbedded with grey fine to medium sandstone package. Orange to deep green amber fragment is embedded in the grey sandstone close to dark coal layers (See bed number 21 in Figure 10).

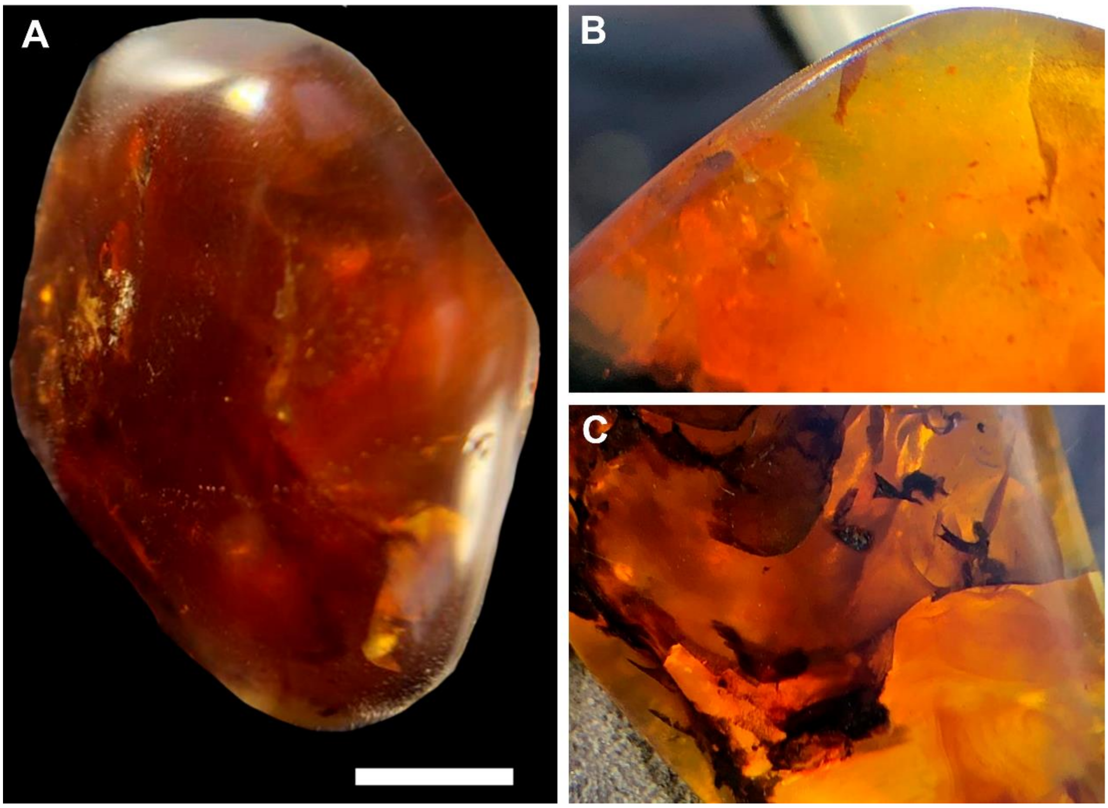

Figure 27. Polished amber samples from the amber collection of Genoveva Mine. A) Brown reddish piece of amber. Scale bar 20 mm. B) Light orange amber with inclusions and microbubbles. C) Amber with conchoidal fractures and oil stain intrusions. Photograph: Dr. Camila Martínez.

6 DISCUSSION

6.1 Stratigraphic and Sedimentological Data.

6.1.1 Interpretation

6.1.1.1 Sedimentary Structures

We used a similar facies code proposed by Miall (1978). He established a relation between the sedimentary structures and lithology for interpretation (Table 5). We apply that relationship as a guide in order to define the sedimentary facies and environment, but not strictly because they are not a universal panacea for sorting out the complexity of fluvial deposits. For that, interpretations that are shown in Table 2, Table 3 and Table 4; consider other factors as lithology, texture, plant remains, paleocurrents in order to estimate the environments and sub-environments.

6.1.1.2 Siltstones

The siltstones are present in all localities studied, but with more frequency in the abandoned Genoveva Mine reaching 41% of the total length of the graphic log (Figure 29), whereas the Pungarayacu and Genoveva Mine contain 12% and 13%, respectively.

The thickness of siltstones is variable. Some siltstones from 1-10 cm of thickness, parallel laminated and ripple structures were registered. Besides, some layers record plant debris. These fine deposits can be the result of settle out of suspension from floodwaters carried into the floodplain, which may form an ephemeral shallow lake that commonly contains considerable plant debris (Boggs Jr., 2006). We attribute these deposits to overbank deposits.

Thicker siltstones package between 2-6 meters were registered in beds number 10,36,37,38 from Genoveva Mine (Figure 10) and beds number 8,15,22,23,25,26 from Abandoned Genoveva Mine (Figure 13). Besides parallel lamination, and ripple structures; the siltstones registered coal, amber clasts, plant remains and pyrite concretions. For instance, plant remains found in bed numbers 36,37,38 from Genoveva Mine could suggest the existence of a deep lake due to the anoxia conditions at the bottom of the lake prevents the aerobic breakdown of organic material that settles on the lake floor, allowing the accumulation of organic-rich sediments (Nichols, 2009). Another fact is the presence of pyrite concretions (Figure 28), which form under euxinic conditions with a contribution of organic matter (López et al., 2009).

Figure 28. Pyrite concretion found in layer 37 from the stratigraphic log of Genoveva mine. Scale bar 2 cm long.

A remarkable point to establish deep lake conditions is the presence of rip-up clasts above the 6 meters siltstone package (Figure 9B). In continental settings, as a fluvial environment, the rip-up silt clasts are interpreted as the result of denser river currents that entered a standing body of water -the lake-, eroding the bottom deposits and transporting sandy and silty clastic particles in bedload and suspension processes, with similar processes as cited by Zavala & Shuxin, (2018), and (Shanmugam, 2018). Thus, the sediments of layers 40,41,49 of Genoveva Mine (Figure 10) can be associated with hyperpycnal flows under lacustrine environments.

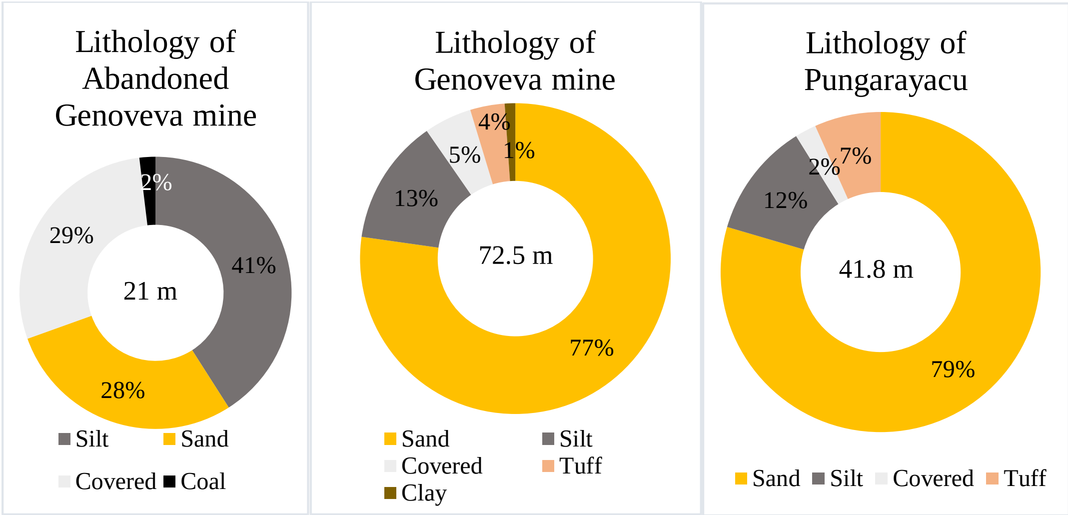

Figure 29. Lithology percentage pie chart from sediments at abandoned Genoveva Mine, Genoveva Mine, and Pungarayacu outcrops.

6.1.1.3 Sandstones

The lithology of the Pungarayacu and Genoveva Mine is strongly dominated by quartz-rich sands (Q ≥ 95 %, Quiroz et al., 2020), reaching 77% – 79% of the total length of the graphic logs (Figure 29). The amount of sandstone packages can be interpreted as a high sediment discharge from a fluvial system (James & Dalrymple, 2010; White et al., 1995). The sedimentary structures present in these sandstones are basal erosive surfaces, planar cross-bedding, trough cross-bedding, ripples currents - which are the result of bedform migration driven by the flow of water or wind (Xu et al., 2015), and parallel lamination formed at high flow velocity, and shallow water depth conditions (Nichols, 2009).

In Abandoned Genoveva Mine, we reported massive and parallel laminated fine to very fine sandstones. Under floodplain conditions, water flow can use crevasse channels to form lacustrine deltas (Aslan, 2013). Thus, due to the parallel lamination, lithology, and coal, we attribute these sandstones into a deltaic environment including delta plain, delta lobe, and delta front facies. This proximal sub-aqueous lacustrine delta has important development of bedload processes such as traction and fall-out.

Table 5. Lithofacies and sedimentary structures of modern and ancient braided stream deposits (Miall, 1978, Table III).

Facies Code	Lithofacies	Sedimentary structures	Interpretation
Gms	massive, matrix supported gravel	none	debris flow deposits
Gm	massive or crudely bedded gravel	horizontal bedding, imbrication	longitudinal bars, lag deposits, sieve deposits
Gt	gravel, stratified	trough crossbeds	minor channel fills
Gp	gravel, stratified	planar crossbeds	linguoid bars or deltaic growths from older bar remnants
St	sand, medium to v. coarse, may be pebbly	solitary (theta) or grouped (pi) trough crossbeds	dunes (lower flow regime)
Sp	sand, medium to v. coarse, may be pebbly	solitary (alpha) or grouped (omikron) planar crossbeds	linguoid, transverse bars, sand waves (lower flow regime)
Sr	sand, very fine to coarse	ripple marks of all types	ripples (lower flow regime)
Sh	sand, very fine to very coarse, may be pebbly	horizontal lamination, parting or streaming lineation	planar bed flow (l. and u. flow regime)
Sl	sand, fine	low angle (<10°) crossbeds	scour fills, crevasse splays, antidunes
Se	erosional scours with intraclasts	crude crossbedding	scour fills
Ss	sand, fine to coarse, may be pebbly	broad, shallow scours including eta cross-stratification	scour fills
Sse, She, Spe	sand	analogous to *Ss, Sh, Sp*	eolian deposits
Fl	sand, silt, mud	fine lamination, very small ripples	overbank or waning flood deposits
Fsc	silt, mud	laminated to massive	backswamp deposits
Fcf	mud	massive, with freshwater molluscs	backswamp pond deposits
Fm	mud, silt	massive, desiccation cracks	overbank or drape deposits
Fr	silt, mud	rootlets	seatearth
C	coal, carbonaceous mud	plants, mud films	swamp deposits
P	carbonate	pedogenic features	soil

6.1.1.4 Texture

In general, all graphic logs present both textural tendencies: coarsening-upward (from fine to coarse-grained) and fining-upward (from coarse to fine-grained), represented as arrows in these sedimentary logs. These changes are explained due to seismic activity and strong volcanic activity own from the Ecuadorian Sub-Andean Zone (Baby et al., 2004).

6.1.1.5 Paleocurrents

Sedimentary structures can be used to interpret depositional environments and ancient hydraulics. Among them, one of the most valuable pieces of data is the flow direction indicated by unidirectional or bidirectional currents (Prothero & Schwab, 2014). The majority of paleocurrents data from cross-stratified sandy packages in Pungarayacu outcrop and Genoveva Mine indicate three general flow direction patterns: from South to North; from SE to NW; from SSW to NNW; and from SW to NE (Figure 30).

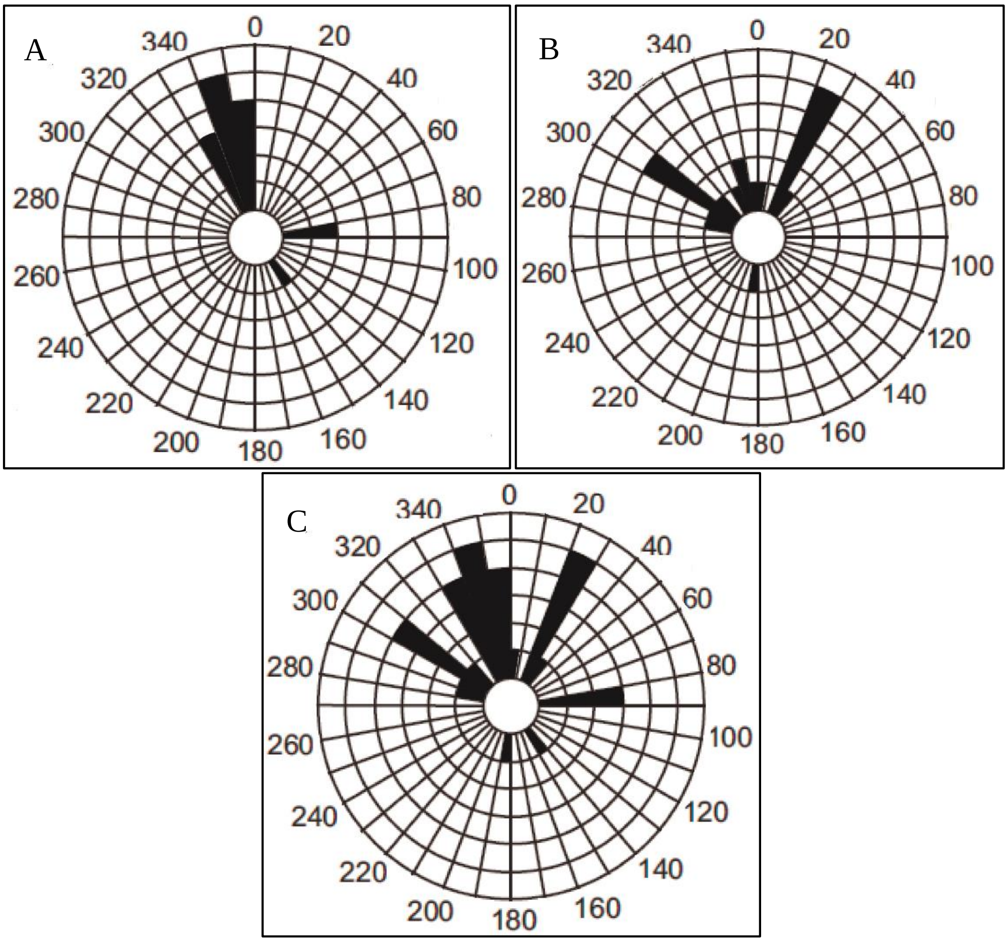

Figure 30. A) Paleocurrents from Genoveva Mine. B) Paleocurrents from Pungarayacu Outcrop. C) Paleocurrents from both Genoveva Mine and Pungarayacu Outcrop.

6.1.2 Discussion

Facies like fluvial channel, fluvial plain, fluvial bar, and mouth bar are properly from braided fluvial systems, whereas hyperpycnal flows, bay, inner lake, outer lake, delta, and beach facies can be associated with lacustrine deposits (Boggs Jr., 2006; Nichols, 2009; Posamentier & Walker, 2006; Reading, 1996) and nearshore sediments. Consequently, the sediments and facies from the three localities: Pungarayacu outcrop, Genoveva Mine, and abandoned Genoveva Mine correspond to a braided river and lacustrine deposits of the Lower Hollin Formation.

Within this system, three major depositional environments were established.

1. Pyroclastic.

Located at the base of the Pungarayacu outcrop and Genoveva Mine (Figure 6 and Figure 10), this volcanogenic environment is characterized by an accumulation of volcano-pyroclastic particles of ash, lapilli, and pumice into a poorly consolidated volcano-sedimentary matrix, eventually forming an altered tuff. Base on that, two lithofacies were defined: (1) Pyroclastic flows; and (2) Paleosoil.

Romeuf et al. (1995) described similar features outcropping in central and southern SAZ of Ecuador that corresponds to the Misahualli Volcanics. It consists mainly of basaltic to rhyolitic lava flows and acid pyroclastic deposits that were erupted in a subaerial environment. Radiometric analysis ^{40}Ar ^{39}Ar estimate an approximate age of 172 Ma.

2. Braided stream rivers

Previous authors (Baby et al., 2004; Dashwood & Abbotts, 1990; Shanmugam et al., 2000; White et al., 1995) described Braided stream river and distal Coastal alluvial plain deposits within the Lower Hollin Formation. Particularly, they described braided rivers defined by planar and trough cross-bedding sets are interpreted as straight mid-channel bars; and interbedded mudstone and sandstone attributed as channels, overbank levee, and crevasse. Although the river discharge may have been seasonally variable, the sand bedload discharge was sufficiently high to account for the stacked braid bars. Similar type of sediments were described in this research project. Massive, planar-laminations, through and planar cross-bedding in medium-to fine-grained sandstone packages are indicative of fluvial channels; medium to fine parallel-laminated, medium- to fine-grained sandstones corresponds to fluvial plains; fine to coarse parallel-laminated or planar cross-bedding with ripple marks can be associated to fluvial bars.

Amber, coal, and plant remains were reported in Upper Hollin Formation (Romero Condor, 2018; Shanmugam et al., 2000). These organic materials are accompanied by specific sedimentary structures like flaser-bedding, rhythmites, double mud layers, wavy bedding, lenticular bedding, and crinkle laminae. In the localities studied in this research project, within the facies corresponding to Lower Hollin Formation, we also found grains of amber, coal laminations and beds, and plant remains, but with the absence of tidally-generated sedimentary structures.

3. Lacustrine environment

Siltstones packages are present in all graphic logs constructed in this project, but more recurrent to the West of the study area, that is, in the surroundings of the Genoveva area. They can be inferred as: (1) Shallow lakes forming overbank deposits and (2) Deep lake facies.

The sedimentary facies associated with the overbank sub-environment in this project are thin shales, silty shales and silts, composing the lithofacie of laminated sand, silt, and mud (Fl) with few plant remains. According to Aslan (2013), under humid conditions, flood basins are vegetated and contain lakes and perennial or seasonal wetlands, which coincides to our interpretation. However, the author also mentions that it is common to find mudcracks and bioturbations in this sub-environment, but we do not find them on the field.

Thick 2 to 6 meters silty to shale sediments constitute Outer and Inner Lake facies. Boggs Jr. (2006) states that deeper parts of the lake are characterized particularly by the presence of fine silt and clay, as the facies found in Genoveva Mine (Figure 10). These sediments could be concentrated in topographic depressions where water levels are perennially elevated and reducing conditions prevail. These deposits often contain reducing minerals such as pyrite, vivianite, and jarosite (Aslan, 2013). In the case of Genoveva Mine, we reported pyrite concretions whereby we can affirm that pyrite concretions were formed under reducing conditions in a deep lake environment. Nonetheless, varves are one of the more diagnostic characteristic of lake sediments, and we cannot find them on the field due to the oil staining present in sediments.

6.2 Fossil Taxa

In total, twenty-two morphotypes have been identified (Table 6) in this project. Seven cuticle morphotypes collected in Pungarayacu were defined from which two morphotypes correspond to Cupressaceae and Podocarpaceae families, two are possibly associated with angiosperms, and three remain unidentified. The leaf macrofossils collected in the Genoveva Mine and abandoned Genoveva Mine were grouped in fifteen morphotypes from which Cupressaceae, Podocarpaceae, ferns, possible Cycadales, and angiosperms can be defined.

6.2.1 Current plants in the study areas

Currently, the studied localities correspond to the Sub-Andean evergreen forest of the west Amazon basin of Ecuador. These forests are characterized by reaching a canopy height of 30 meters (Lozano, 2011). Over 1000 meters, the forests are entirely dominated by angiosperms like *Billia rosea* (Sapindaceae), *Minquartia guianensis* (Coulaceae), *Compsoneura ulei, Otoba glycycarpa, Virola* spp. (Myristicaceae), *Dacryodes olivifera* (Burseraceae), *Hieronyma macrocarpa* (Phyllanthaceae), *Pseudolmedia rigida* (Moraceae), *Grias neuberthii* (Lecythidaceae), *Wettinia anomala* (Arecaceae). In the understory, the families present are Melastomataceae and Rubiaceae, but it is common to find palms like *Geonoma* spp. and *Hyospathe elegans (*Arecaceae) (Ministerio del Ambiente del Ecuador, 2012). The abundance of angiosperm is attributed to a positive feedback. Higher growth rates profit angiosperms, since they consume a higher nutrient supply than gymnosperms, and at the same time, promote soil nutrient release by producing litter that is more easily decomposed (Berendse & Scheffer, 2009).

6.2.2 Discussion

Several studies from Early Cretaceous tropical flora from northern South America (Table 1), denote the strong dominance of gymnosperms, ferns and, few angiosperms. In Ecuador, Shoemaker (1982) reported Cycads, Bennettitales, Conifers, and Pinales from the Aptian-Albian Ciano Formation. The results of this project coincided with previous researches suggesting that the Early Cretaceous Lower Hollin Formation was generally dominated by conifers (Cupressaceae and Podocarpaceae) followed by ferns, cycads, and a few angiosperms.

Cupressaceae originated during the late Permian and began to diversify into seven major lineages during the Triassic (Mao et al., 2012). By the Cretaceous, their distribution was worldwide. According to vegetative and reproductive features of the fossils, the modern genera (Callitroideae and Cupressoideae) represent a small part of what must have been a dominant component of the Mesozoic conifer flora (Mao et al., 2012; Taylor et al., 2009).

Podocarpaceae fossils are known from the Lower Triassic and extend throughout the Mesozoic and Cenozoic (Taylor et al., 2009). They are still present in the Ecuadorian flora, constituting the most abundant species in the Podocarpus National Park located in southern Ecuador, in Loja and Zamora Chinchipe provinces. This area is home to moors, cloud forests, and scrubs, essential for the preservation and continuity of the ecosystems (Sistema Nacional de Áreas Protegidas del Ecuador, 2015).

Another organic remain found in the Genoveva Mine is the fossil resin, best known as amber, which usually encloses biological structures. Some plants exude copious volumes of resin (gum) from their bark, cones, branchlets, and leaves in response to disease, insect infestation, an ecological change, disaster, or fire (Salmon, 1981, *in*: Shanmugam, 1985). Then, the resin solidifies through polymerization, and after deposition, undergoes maturation to become amber (Seyfullah et al., 2018). Currently, angiosperms and gymnosperms tend to exude resin but certainly, during the Cretaceous, conifers were likely the major contributors of resin since angiosperms were not the dominant group (Grimaldi, 1996).

The amber collected from Genoveva Mine is particularly interesting because, together with samples from Araripe Basin from Brazil, they are one of the few cases of Early Cretaceous amber in South America (Gomez et al., 2007).

Approximately 2000 samples were analyzed, which contain oil intrusions and microbubbles but no biological inclusions. We propose two hypotheses that could explain the absence of organic remains in amber: (A) Resin in underground conditions; and (B) Resin under aerial conditions.

A. Resin in underground conditions.

In some cases, the resin is produced by roots as a defense against fungal attacks (Speranza et al., 2015). A braided river system has been defined as one of the paleoenvironments of sediments outcropping in the Genoveva Mine. Hence, we could expect flooding events that can expose the roots and resin to the surface. Then, the resin and plant remains are buried, and under diagenetic conditions, the resin could solidify within the soil and become amber (Figure 31A).

B. Resin under aerial conditions

It is also probable that the resin could have been produced by branches of trees that were located close to water bodies (Seyfullah et al., 2018). Subsequently, by gravity, the resin can fall into the water and be rapidly transported, avoiding contact with organisms like leaves or insects. The resin bodies floated down rivers until arriving at a depositional zone. Then, by diagenesis, the resin became amber (Figure 31B).

In both cases, the final stage is the same, the consolidation of amber that will be found close to plant remains that eventually became coal deposits.

Table 6. Systematic affinity of morphotypes identified in Early Cretaceous Lower Hollin Formation.

Morphotypes	***Systematic Affinity***						
	Cupressaceae	**cf. Angiosperm**	**Podocarpaceae**	**Cycadales**	**Fern**	**Selaginellaceae**	**Unknown**
HF01	X						
HF02		X					
HF03		X					
HF04							X
HF05			X				
HF06							X
HF07							X
HF08				X			
HF09	X						
HF10	X						
HF11	X						
HF12			X				
HF13					X		
HF14					X		
HF15					X		
HF16					X		
HF17					X		
HF18						X	
HF19		X					
HF20		X					
HF21		X					
HF22		X					

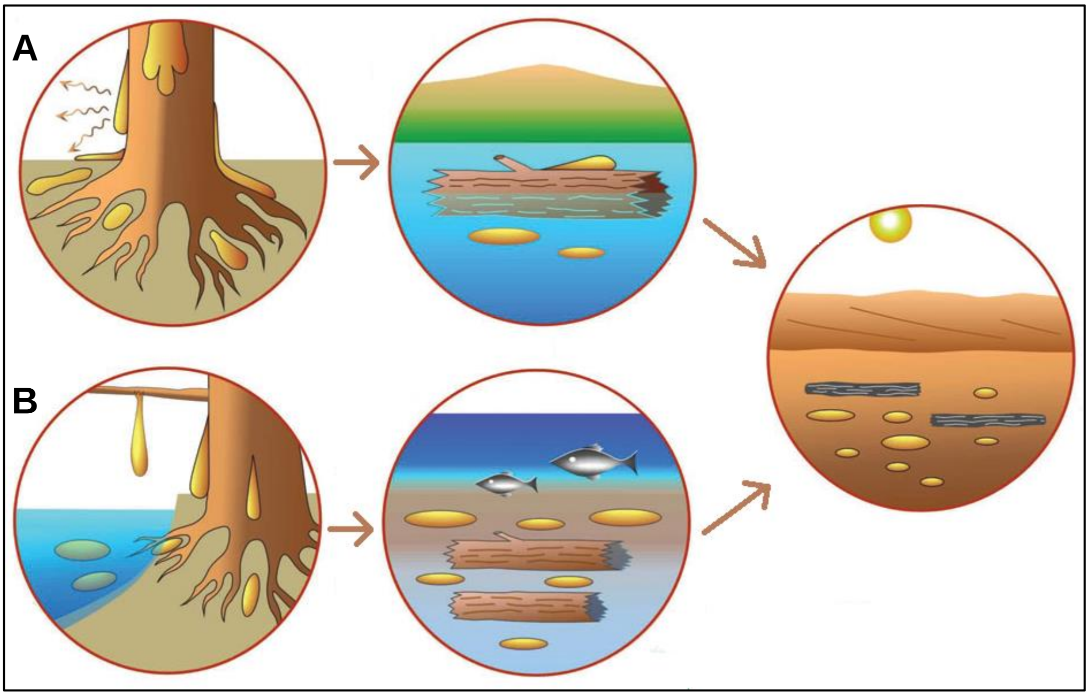

Figure 31. Graphic representation of two hypotheses that can explain the absence of organic remains inside amber from Genoveva Mine. A) Resin in underground conditions. B) Resin under aerial conditions. Modified after Seyfullah et al. (2018).

6.3 Paleoenvironmental Reconstruction

Based on stratigraphic and sedimentological evidence, and the taxonomic composition of the macroflora, the Lower (?) Aptian – middle Albian Lower Hollin Formation of the central Eastern SAZ of Ecuador, was deposited in terrestrial and fluvio-lacustrine environments, particularly in a braided river system, with ephemeral lakes (Figure 32A) and perennial lakes (Figure 32B), surrounded by forests dominated by conifers, ferns, cycads, and a few early angiosperms.

Plant remains collected in Pungarayacu outcrop might be allochthonous due to their fragmented condition and small size, suggesting that they could have been transported over moderate distances. On the other hand, plant macrofossils collected in the Genoveva Mine evidence a little transport before burial due to the good and almost complete preservation of the fossils. Hence, we can assume that they may come from a nearby source. Therefore, the plants maybe recorded a mixture from different sources given the wide of braided rivers belt in this zone.

A

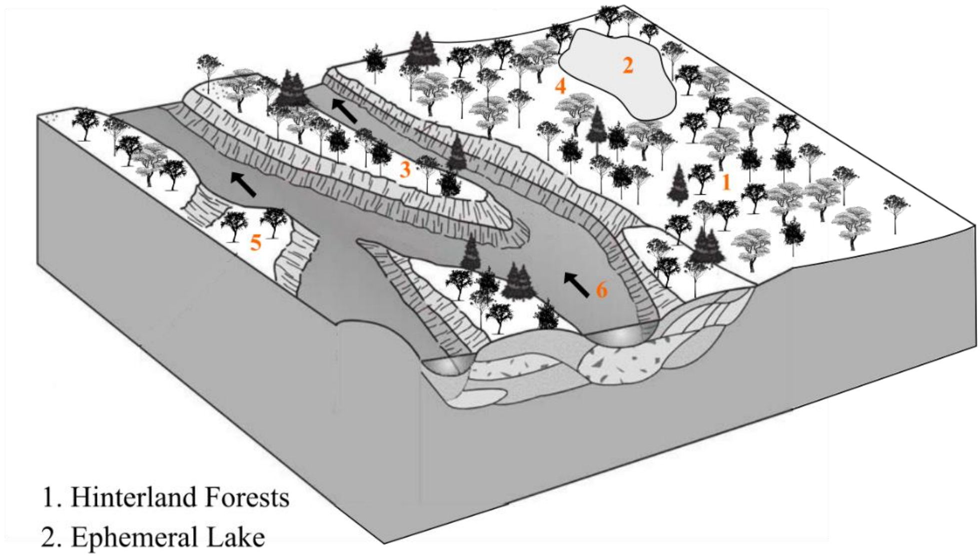

B

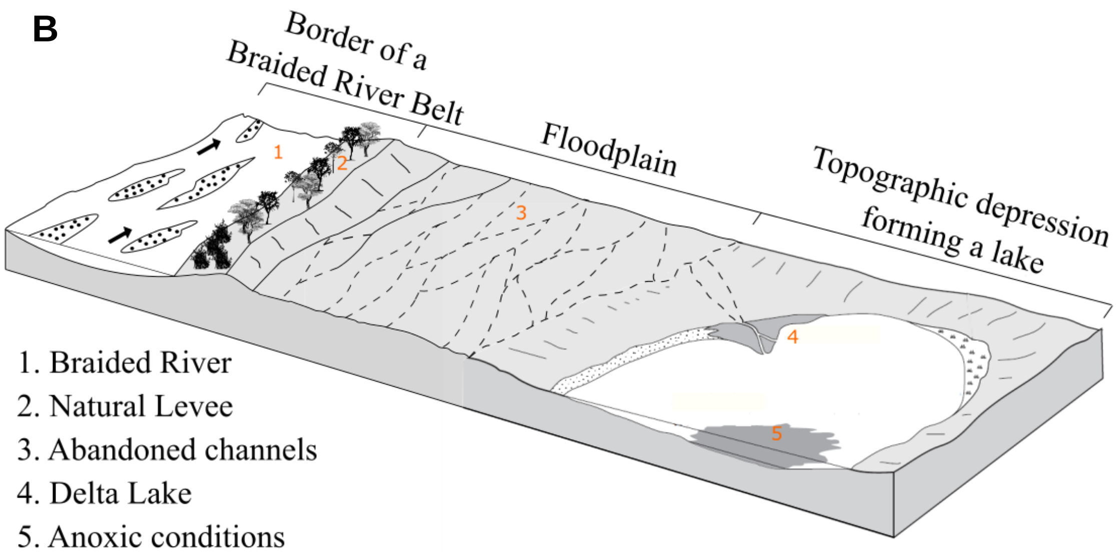

Figure 32. A) Paleoenvironmental reconstruction of braided river system of Lower Hollin Formation. Modified after Prothero & Schwab (2004). B) Paleoenvironment reconstruction from lacustrine environments formed by massive flooding events. Modified after (G. Nichols, 2009).

6.4 Paleoclimate estimation

Jaillard et al. (1997) conducted, among other studies, palynological analyses in the Lower Hollin Formation. They mentioned species as *Classopolis echinatus, Sofrepites legouxae, Cicatricosisporites hallei, Perotriletes pannuceus, Inaperturopollenites simplex, Araucariacites australis, Ephedripites irregularis, Reyrea polymorpha, Ephedripites barghoorni.* According to Herngreen, (1996) Classopollis sp., ephedroid pollen, and elater-bearing species are associated with arid climates. However, Mejia-Velasquez et al. (2012, 2018) reported humid conditions for western South America based on palynological indicators collected from Early Cretaceous stratigraphic successions in Colombia and Peru.

Coal beds found in tropical belt localities are associated with wet environments and provide strong evidence for former tropical rain forest climates (Mejia-Velasquez et al., 2012; Morley, 2000). In this project, we reported coal layers in the Genoveva Mine and abandoned Genoveva Mine; thus, we can infer humid conditions during the deposition of the Lower Hollin Formation. In addition, the presence of ferns is indicative of humid climate instead of arid (Jaramillo, 2012).

Additionally, considering the recurrence of silty to shaley facies packages identified in the study area, interbedded in the sections at Genoveva Mine, Old Genoveva Mine, and Pungarayacu outcrop, composing fluvial plain, delta plain (with plant debris & coal) and lacustrine paleoenvironment (with amber and plant debris), we could infer a humid environment, with frequent episodes of flooding, in which clay-rich clastic sediments were transported from the continent (braided rivers, fluvial plain, delta plain) into the silty to shaley depositional areas (lakes).

The determination of climate from the localities corresponding to the Lower Hollin Formation remains unknown. However, following the evidence presented and researches from Aptian – Albian localities near the equator, we can infer humid conditions in a temperate to warm environment for the current central Eastern SAZ of Ecuador. This statement could be corroborated with palynological studies in the study areas.

7 CONCLUSIONS

- Based on the stratigraphic and sedimentological analysis applied to the three localities in the central eastern Sub-Andean Zones (SAZ) of Ecuador: Pungarayacu outcrop, Genoveva Mine, and abandoned Genoveva Mine, we have determined that the sediments analyzed correspond to sandy to shaley fluvial to lacustrine deposits associated with braided stream rivers systems of Lower Hollin Formation. The age is Lower Aptian (?) – Middle Albian, and unconformable overly Upper Jurassic of volcanoclastic sediments (Misahualli Volcanics).
- The floristic composition defined by cuticle remains and leaf macrofossils suggest an environment strongly dominated by gymnosperms like Cupressaceae and Podocarpaceae conifers, ferns as Selaginella, and few angiosperms. Given the conditions of preservation of fossils, very fragmented cuticles, and well-preserved leaf macrofossils, we can estimate different levels of transportation of organic matter in the western Oriente basin.
- The amber fragments found in the sediments of Genoveva Mine do not contain any animal organic remains, probably due to underground resin production or fast-cooling resin produced by dripping into a body of water.
- In terms of paleoclimate, given: (1) the coal laminations and layers associated with swamps; (2) the variable percentage of silty to shaley lake sediments in the analyzed outcrops (41% to the west, in the abandoned Genoveva Mine, and 12% to the east, in the Pungarayacu outcrop); and (3) the previous palynological studies developed in Early Cretaceous near equatorial areas, we can assume humid conditions in a temperate to warm environment, with coniferous rain forests dominating, for the deposition of the Lower Hollin Formation, in the area of the current central Eastern SAZ of Ecuador.

Integrated studies of leaf macrofossils, CO_2 estimation based on stomata distribution, and pollen analysis from these stratigraphic successions in Central Eastern SAZ will provide a complete vegetational reconstruction.

ANNEX 1

STRATIGRAPHIC LOF OF PUNGARAYACU OUTCROP

SCALE 1:100

Graphic Log of Pungarayacu

Scale 1:100

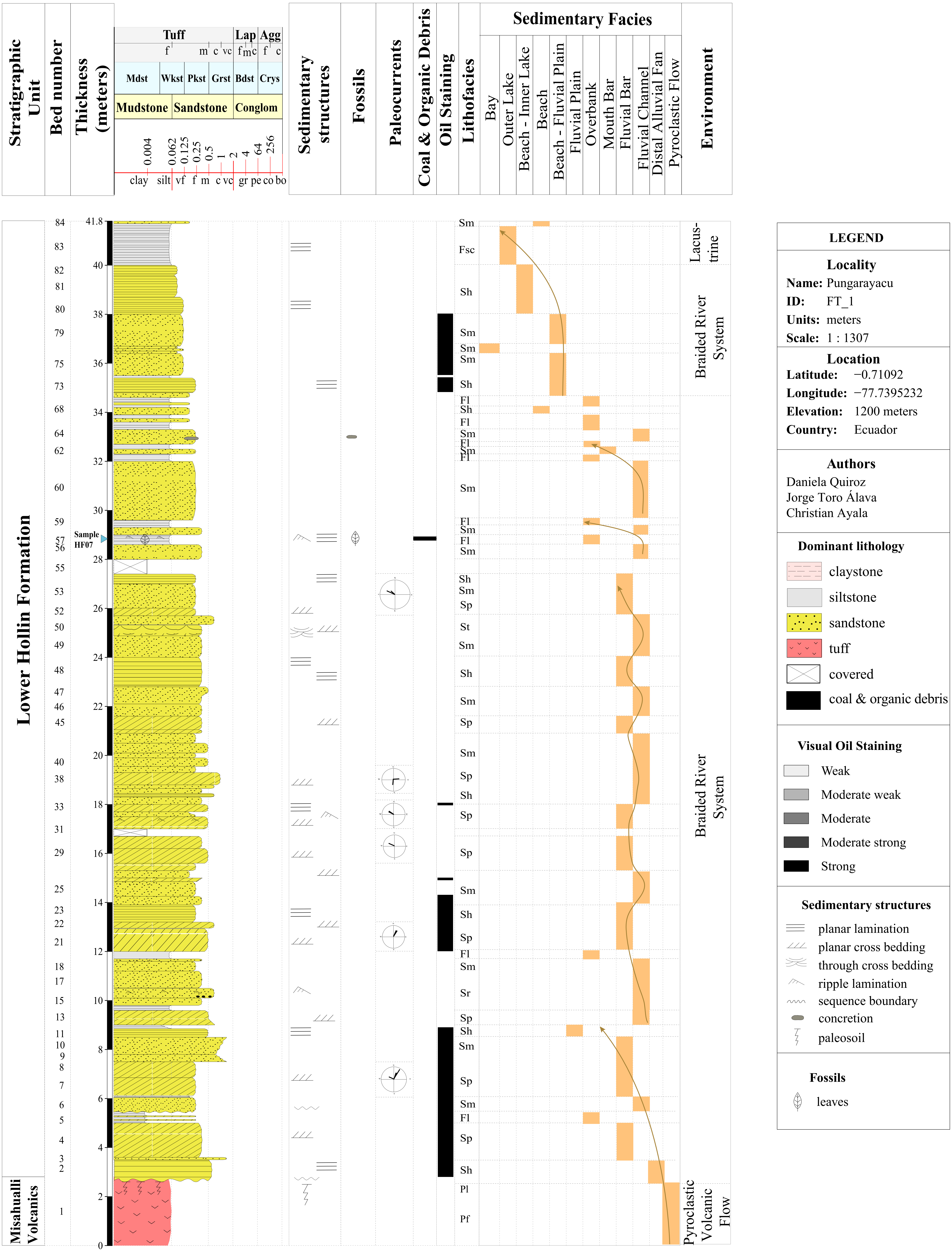

ANNEX 2

STRATIGRAPHIC LOF OF GENOVEVA MINE

SCALE 1:100

Graphic Log of Genoveva Mine

Scale 1:100

ANNEX 3

STRATIGRAPHIC LOF OF ABANDONED GENOVEVA MINE

SCALE 1:100

Graphic Log of Abandoned Genoveva Mine

Scale 1:100

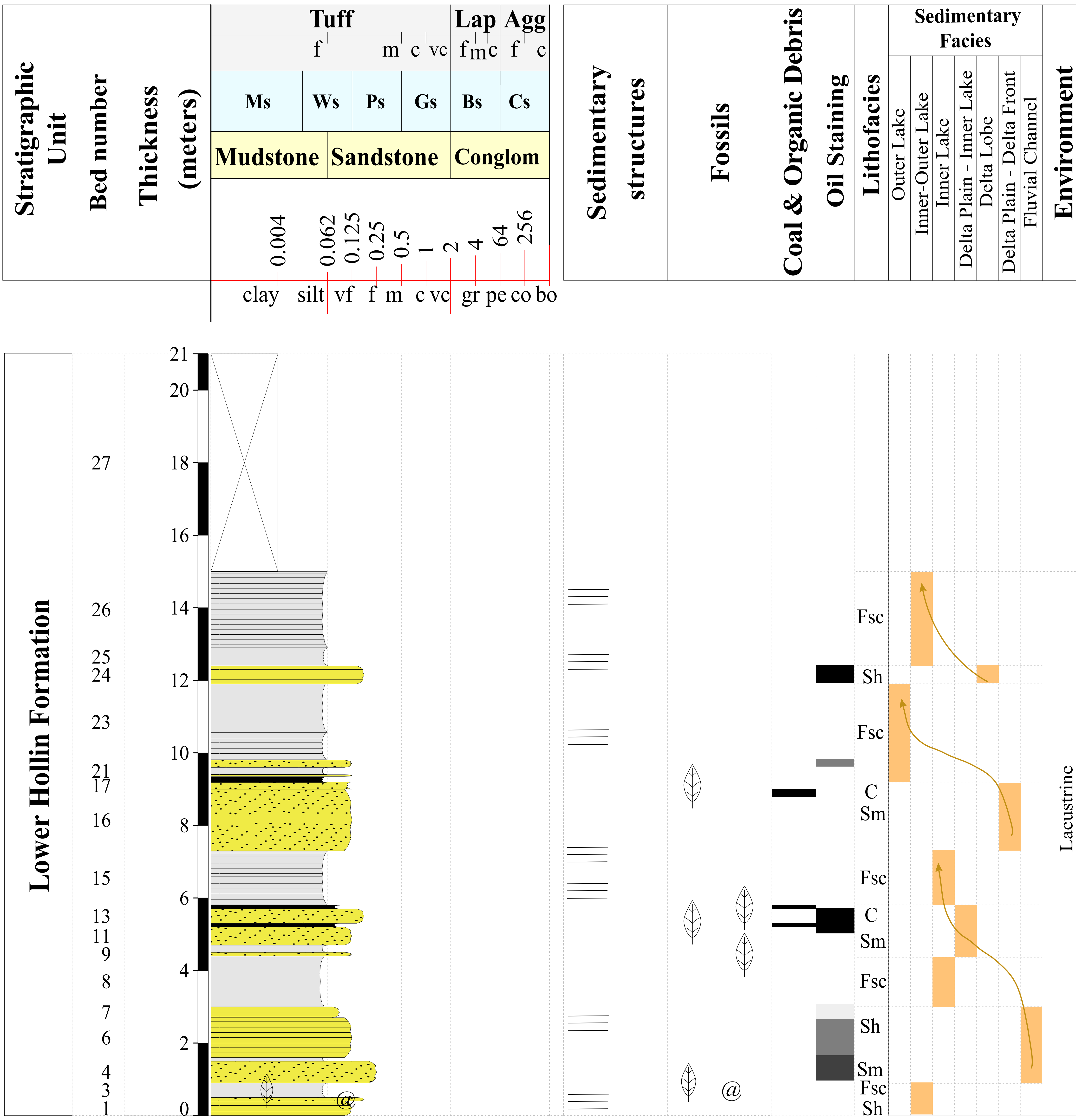

Locality
Name: Abandoned Genoveva Mine
ID: FT1
Units: meters
Scale: 1 : 200

Location
Latitude: −0.711922
Longitude: −77.7909313
Elevation: 1214 meters
Country: Ecuador

Authors

Daniela Quiroz
Jorge Toro Álava

LEGEND

Dominant lithology

- siltstone
- sandstone
- coal & organic debris
- covered

Visual Oil Staining

- Weak
- Moderate weak
- Moderate
- Moderate strong
- Strong

Sedimentary structures

- planar lamination

Fossils

- leaves
- @ amber

REFERENCES

Antonelli, A., & Sanmartín, I. (2011). Why are there so many plant species in the Neotropics? *Taxon*, *60*(2), 403–414. https://doi.org/10.1002/tax.602010

Aslan, A. (2013). Fluvial Environments | Sediments. In S. A. Elias & C. J. Mock (Eds.), *Encyclopedia of Quaternary Science (Second Edition)* (Second Edi, pp. 663–675). Elsevier. https://doi.org/https://doi.org/10.1016/B978-0-444-53643-3.00111-4

Baby, P., Rivadeneira, M., & Barragán, R. (2004). *La cuenca Oriente: geología y petróleo* (Vol. 144). Institut français d'études andines.

Battarbee, R. W., Jones, V. J., Flower, R. J., Cameron, N. G., Bennion, H., Carvalho, L., & Juggins, S. (2002). Diatoms. In *Tracking environmental change using lake sediments* (pp. 155–202). Springer.

Berendse, F., & Scheffer, M. (2009). The angiosperm radiation revisited, an ecological explanation for Darwin's "abominable mystery." *Ecology Letters*, *12*(9), 865–872. https://doi.org/10.1111/j.1461-0248.2009.01342.x

Boggs, Jr. S. (2006). *Principles of sedimentology and stratigraphy* (4th ed.). Pearson Prentice Hall.

Burnham, R. J., & Johnson, K. R. (2004). South American palaeobotany and the origins of neotropical rainforests. *Philosophical Transactions of the Royal Society of London. Series B: Biological Sciences*, *359*(1450), 1595–1610. https://doi.org/10.1098/rstb.2004.1531

Cadena, E. A., Mejia-Molina, A., Brito, C. M., Peñafiel, S., Sanmartin, K. J., & Sarmiento, L. B. (2018). New Mesozoic and Cenozoic fossils from Ecuador: Invertebrates, vertebrates, plants, and microfossils. *Journal of South American Earth Sciences*, *83*, 27–36. https://doi.org/10.1016/j.jsames.2018.02.004

Christophoul, F., Baby, P., & Dávila, C. (2002). Stratigraphic responses to a major tectonic event in a foreland basin: the Ecuadorian Oriente Basin from Eocene to Oligocene times. *Tectonophysics*, *345*(1–4), 281–298.

Crang, R., Lyons-Sobaski, S., & Wise, R. (2018). *Plant Anatomy: A concept-based approach to the structure of seed plants*. Springer.

Culver, S. J., & Rawson, P. F. (2004). *Biotic Response to Global Change*. Cambridge

University Press. https://doi.org/10.1017/CBO9780511535505.022

Dark, P. (2008). Paleoenvironmental reconstruction, methods. *Encyclopedia of Archaeology*, *2005*, 1787–1790. https://doi.org/10.1016/B978-012373962-9.00226-0

Dashwood, M. F., & Abbotts, I. L. (1990). Aspects of the petroleum geology of the Oriente Basin, Ecuador. *Geological Society of London*, *50*(1), 89–117.

Domínguez, E., Heredia-Guerrero, J. A., & Heredia, A. (2011). The biophysical design of plant cuticles: an overview. *The New Phytologist*, *189*, 938–949. https://doi.org/10.1111/j.1469-8137.2010.03553.x

Friis, E. M., Crane, P. R., & Pedersen, K. R. (2011). *Early flowers and angiosperm evolution*. Cambridge University Press. https://doi.org/10.1017/CBO9780511980206

Gomez, B., Martínez-Delclos, X., Bamford, M., & Philippe, M. (2007). Taphonomy and palaeoecology of plant remains from the oldest African Early Cretaceous amber locality. *Lethaia*, *35*(4), 300–308. https://doi.org/10.1111/j.1502-3931.2002.tb00090.x

Gradstein, F. M., Ogg, J. G., Schmitz, M. B., & Ogg, G. M. (2012). *The geologic time scale 2012*. Elsevier.

Grimaldi, D. A. (1996). *Amber: window to the past*. Harry N. Abrams, Publishers New York.

Herendeen, P. S., Friis, E. M., Pedersen, K. R., & Crane, P. R. (2017). Palaeobotanical redux: Revisiting the age of the angiosperms. *Nature Plants*, *3*(3), 1–8. https://doi.org/10.1038/nplants.2017.15

Herngreen, G. F. W. (1996). Cretaceous palynofloral provinces : a review. *Palynology : Principles and Applications. American Association of Stratigraphic Palynologists Foundation*, *3*, 1157–1188. https://ci.nii.ac.jp/naid/10003919759

Holmes, J. A. (2001). Ostracoda. In *Tracking environmental change using lake sediments* (pp. 125–151). Springer. https://doi.org/https://doi.org/10.1007/0-306-47671-1_7

Huertas, G. (1970). Sertum florulae fossils Villae de Leiva II. *Caldasia*, *10*, 595–602. https://www.jstor.org/stable/23641431?seq=1

Jaillard, E., Caron, M., Dhondt, A., Ordoñez, M., Lascano, M., Andrade, R., Bengtson, P., Bulot, L., Cappetta, H., Dávila, C., Díaz, R., Huamán, C., Jimenez, N., Montenegro, J., Neradau, D., Rivadeneira, M., Toro Alava, J., Villagómez, R., & Zambrano, I. (1997). Síntesis Estratigráfica y Sedimentológica del Cretáceo y Paleógeno de la Cuenca Oriental del Ecuador. In *ORSTOM-Petroproduccion Publication* (Vol. 1).

James, N. P., & Dalrymple, R. W. (Eds.). (2010). *Facies models 4*. Canada: Geological Association of Canada.

Jaramillo, C. (2012). Historia geológica del bosque húmedo neotropical. *Revista de La Academia Colombiana de Ciencias Exactas, Físicas y Naturales*, *36*(138), 57–77.

Jaramillo, C., & Ortiz, J.. (2020). SDAR. doi: 10.25573/data.13118426.v2

Lima, F. J., Saraiva, A. Á. F., & Sayão, J. M. (2012). Revisão da Paleoflora das Formações Missão Velha, Crato e Romualdo, Bacia do Araripe, Nordeste do Brasil. *Estudos Geológicos*, *22*(1), 99–115. https://doi.org/10.18190/1980-8208/estudosgeologicos.v22n1p99-115

López, L., Lo Mónaco, S., Escobar, G., Camargo, C., Lugo, P., Rojas, H., & González, C. (2009). Study of pyrite nodules from Querecual Formation, Anzoátegui state (Venezuela) by with electron probe microanálisis. *Acta Microscopica*, *18*, 333–343.

Lozano, P. (2011). Flora de las estribaciones andinas de la provincia de Napo. Quito: *ECOBONA*, Serie Investigación y Sistematización No. 20. Programa Regional ECOBONA INTERCOOPERATION. Quito.

Mao, K., Milne, R. I., Zhang, L., Peng, Y., Liu, J., Thomas, P., Mill, R. R., & Renner, S. S. (2012). Distribution of living Cupressaceae reflects the breakup of Pangea. *Proceedings of the National Academy of Sciences*, *109*(20), 7793–7798. https://doi.org/10.1073/pnas.1114319109

Mariño Morejón, E. (2016). Identificación y caracterización de facies de la Formación Hollín en un afloramiento ubicado en el Proyecto Hidroeléctrico Coca-Codo Sinclair, provincia de Napo: *Escuela Politécnica Nacional*, Facultad Ingeniería en Geología y Petróleos, Tesis de grado previa la obtención de título de Ingeniero Geólogo, 220 p. más anexos, Quito.

Martill, D. M., Loveridge, R. F., De Andrade, J. A. F. G., & Cardoso, A. H. (2005). An unusual occurrence of amber in laminated limestones: The Crato Formation lagerstätte (Early Cretaceous) of Brazil. *Palaeontology*, *48*(6), 1399–1408. https://doi.org/10.1111/j.1475-4983.2005.00517.x

Martínez, L. C. A., Pacheco Huacallo, E., Pujana, R. R., & Padula, H. (2020). A new megaflora (leaves and reproductive structures) from the Huancané Formation (Lower Cretaceous), Peru. *Cretaceous Research*, *110*. https://doi.org/10.1016/j.cretres.2020.104426

Mejia-Velasquez, P. J., Dilcher, D. L., Jaramillo, C. A., Fortini, L. B., & Manchester, S. R. (2012). Palynological composition of a Lower Cretaceous South American tropical sequence: Climatic implications and diversity comparisons with other latitudes. *American Journal of Botany*, *99*(11), 1819–1827. https://doi.org/10.3732/ajb.1200135

Mejia-Velasquez, P. J., Manchester, S. R., Jaramillo, C. A., Quiroz, L., & Fortini, L. (2018). Floristic and climatic reconstructions of two Lower Cretaceous successions from Peru. *Palynology*, *42*(3), 420–433. https://doi.org/10.1080/01916122.2017.1373310

Miall, A. D. (1978). Lithofacies types and vertical profile models in braided river deposits: a summary. *Fluvial Sedimentology*, *5*, 597–600. http://archives.datapages.com/data/dgs/005/005001/597_cspgsp0050597.htm

Ministerio del Ambiente del Ecuador. (2012). Sistema de clasificación de los ecosistemas del Ecuador continental. *Subsecretaría de Patrimonio Natural*. Quito.

Mohr, B. A. R., & Friis, E. M. (2000). Early angiosperms from the Lower Cretaceous Crato Formation (Brazil), a preliminary report. *International Journal of Plant Sciences*, *161*(S6), S155--S167.

Monje-Dussán, C., Martínez, C., Escapa, I., & Madriñán, S. (2016). Nuevos registros de helechos y coníferas del Cretácico Inferior de la Cuenca del Valle Superior del Magdalena, Colombia. *Boletín de Geología*, *38*(4), 29–42. https://doi.org/10.18273/revbol.v38n4-2016002

Moreno Sánchez, M., Gómez Cruz, A. de J., & Castillo González, H. (2007). Frenelopsis y Pseudofrenelopsis (Coniferales: Cheirolepidiaceae) en el Cretácico Temprano de Colombia. *Boletín de Geología*, *29*(2), 13–19.

Morley, R. J. (2000). *Origin and Evolution of Tropical Rain Forests*. John Wiley & Sons.

Nichols, D. J., & Johnson, K. R. (2008). *Plants and the K-T Boundary*.

Nichols, G. (2009). *Sedimentology and stratigraphy*. John Wiley & Sons.

Peppe, D. J., Hickey, L. J., Miller, I. M., & Green, W. A. (2008). A Morphotype Catalogue, Floristic Analysis and Stratigraphic Description of the Aspen Shale Flora(Cretaceous–Albian) of Southwestern Wyoming. *Bulletin of the Peabody Museum of Natural History*, *49*(2), 181–208. https://doi.org/10.3374/0079-032x-49.2.181

Posamentier, H., & Walker, R. G. (2006). *Facies Models Revisited*. Society for Sedimentary Geology.

Prothero, D., & Schwab, F. (2004). *Sedimentary geology*. W.H. Freeman and Company.

Prothero, D. R., & Schwab, F. (2014). Sedimentary Geology: An Introduction to Sedimentary Rocks and Stratigraphy: *W.H. Freeman & Co.*, third edition, 603 p., NY.

Quiroz, D.E., Ayala, C.O., & Toro Álava, J. (2020), Informe Estratigráfico – Mineralógico de la Concesión Minera Genoveva, cantón Archidona, Ecuador: Yachay Tech University, School of Earth, Energy and Environmental Sciences, Carrera de Geología, & Instituto Smithsonian de Investigaciones Tropicales, reporte técnico de campo para la Concesión Genoveva, campaña del 12 al 30 de enero del 2020, 22 p., Urcuquí-Ecuador.

Reading, H. G. (1996). *Sedimentary environments: processes, facies and stratigraphy* (third). Blackwell Publishing Co., USA.

Romero Condor, C. W. (2018). Identificación y caracterización de facies de la Formación Hollín en el Centro Shaime: El registro de una transición fluvio-marina en la región Sur Oriental del Ecuador: *Escuela Politécnica Nacional*, Facultad Ingeniería en Geología y Petróleos, Tesis de grado previa la obtención de título de Ingeniero Geólogo, 274 p. más anexos, Quito

Romero, E. J. (1993). South American Paleofloras. In *Biological relationships between Africa and South America* (pp. 62–85). Yale University Press: New Haven, CT.

Romeuf, N., Aguirre, L., Soler, P., Féraud, G., Jaillard, E., & Ruffet, G. (1995). Middle

Jurassic volcanism in the Northern and Central Andes . *Andean Geology*, *22*, 245–259. http://www.andeangeology.cl/index.php/revista1/article/view/V22n2-a08/1739

Schoemaker, R. E. (1982). Fossil leaves from the lower Cretaceous Ciano Formation, southwestern Ecuador. *Palaeontographica Abteilung B-Palaophytologie*, *180*, 120–132.

Seyfullah, L. J., Beimforde, C., Dal Corso, J., Perrichot, V., Rikkinen, J., & Schmidt, A. R. (2018). Production and preservation of resins - past and present. *Biological Reviews*, *93*(3), 1684–1714. https://doi.org/10.1111/brv.12414

Shanmugam, G. (1985). Significance of Coniferous Rain Forests and Related Organic Matter in Generating Commercial Quantities of Oil, Gippsland Basin, Australia. *AAPG Bulletin*, *69*(8), 1241–1254.

Shanmugam, G., Poffenberger, M., & Toro Álava, J. (2000). Tide-dominated estuarine facies in the Hollin and Napo ("T" and 'U') formations (Cretaceous), Sacha field, Oriente basin, Ecuador. *AAPG Bulletin*, *84*(5), 652–682. https://doi.org/10.1306/c9ebce7d-1735-11d7-8645000102c1865d

Shanmugam, G. (2018). The hyperpycnite problem. *Journal of Palaeogeography*, *7*(1), 1–42.

Shuman, B. N. (2013). Paleoclimate Reconstruction: Approaches. In *Encyclopedia of Quaternary Science: Second Edition* (pp. 179–184). Elsevier Inc. https://doi.org/10.1016/B978-0-444-53643-3.00008-X

Sistema Nacional de Áreas Protegidas del Ecuador. (2015). *Parque Nacional Podocarpus* http://areasprotegidas.ambiente.gob.ec/es/areas-protegidas/parque-nacional-podocarpus

Smith, L. R. (1989). Regional variations in formation water salinity, Hollin and Napo Formations (Cretaceous), Oriente Basin, Ecuador. *AAPG Bulletin*, *73*(6), 757–776. https://doi.org/10.1306/44b4a258-170a-11d7-8645000102c1865d

Speranza, M., Delclòs, X., & Peñalver, E. (2015). Cretaceous mycelia preserving fungal polysaccharides: Taphonomic and paleoecological potential of microorganisms preserved in fossil resins. *Geologica Acta*, *13*(4), 363–385. https://doi.org/10.1344/GeologicaActa2015.13.4.8

Taylor, E. L., Taylor, T. N., & Krings, M. (2009). *Paleobotany: the biology and evolution of fossil plants*. Academic Press.

Tschopp, H. J. (1953). Oil explorations in the Oriente of Ecuador. *AAPG Bulletin*, *37*(10), 2303–2347.

Vallejo, C., Hochuli, P. A., Winkler, W., & von Salis, K. (2002). Palynological and sequence stratigraphic analysis of the Napo Group in the Pungarayacu 30 well, Sub-Andean Zone, Ecuador. *Cretaceous Research*, *23*(6), 845–859. https://doi.org/10.1006/cres.2002.1028

Van Cotthem, W. R. J. (1970). A classification of stomatal types. *Botanical Journal of the Linnean Society*, *63*(3), 235–246. https://doi.org/10.1111/j.1095-8339.1970.tb02321.x

van Waveren, I. M., van Konijnenburg-van Cittert, J. H. A., van der Burgh, J., & Dilcher, D. L. (2002). Macrofloral remains from the Lower Cretaceous of the Leiva region (Colombia). *Scripta Geologica*, *123*, 1–22.

Villagomez, R., Jaillard, E., Bulot, L., Rivadeneira, M., & Vera, R. (1996). The Aptian - Late Albian marine transgression in the Oriente Basin of the Ecuador: *Troisième symposium international sur la Géodynamique andine*, ORSTOM Éds., Collection Colloques et Séminaires, Saint-Malo (France), du 17 au 19 septembre 1996, Résumés étendus, pp. 521-524, France.

Von Der Osten, E. (1957). Lower Cretaceous Barranquin Formation of northeastern Venezuela. *AAPG Bulletin*, *41*(4), 679–708.

Wasson, H & Sinclair, H. J. (1927). Geological Explorations East of the Andes in Ecuador. *AAPG Bulletin*, *111*(12), iii. https://doi.org/10.1126/science.59.1514.12-a

White, H. J., Skopec, R. a, Ramirez, F. a, Rodas, J. a, & Bonilla, G. (1995). Reservoir characterization of the Hollin and Napo Formations, western Oriente basin, Ecuador. *Petroleum Basins of South America*, *62*, 573–596. http://search.datapages.com/data/specpubs/memoir62/30white/0573.htm

Willis, K., & McElwain, J. (2014). *The evolution of plants*. Oxford University Press.

Xu, C., Gehenn, J. M., Zhao, D., Xie, G., & Teng, M. K. (2015). The fluvial and lacustrine sedimentary systems and stratigraphic correlation in the Upper Triassic Xujiahe Formation in Sichuan Basin, China. *AAPG Bulletin*, *99*(11), 2023–2041.

https://doi.org/10.1306/07061514236

Yeats, T. H., & Rose, J. K. C. (2013). The formation and function of plant cuticles. *Plant Physiology*, *163*(1), 5–20. https://doi.org/10.1104/pp.113.222737

Zavala, C., & Pan, S. (2018). Hyperpycnal flows and hyperpycnites: Origin and distinctive characteristics. *Lithologic Reservoirs*, *30*(1), 1–27. https://doi.org/10.3969/j.issn.1673-8926.2018.01.001